THE PRE-FEASIBILITY STUDY FOR THE SAN KAMPAENG GEOTHERMAL DEVELOPMENT PROJECT IN THE KINGDOM OF THAILAND

TECHNICAL REPORT

(THE 1st AND 2nd PHASE STUDY)

JANUARY, 1984

JAPAN INTERNATIONAL COOPERATION AGENCY

THE PRE-FEASIBILITY STUDY FOR THE SAN KAMPAENG GEOTHERMAL DEVELOPMENT PROJECT IN THE KINGDOM OF THAILAND TECHNICAL REPORT (THE 1st AND 2nd PHASE STUDY)

1. TECHNICAL REPORT

2. TABLE FOR MAPS

(1) PL II.1.1-1 Geological Map
(2) PL II.1.1-2 Geological Profile
(3) PL II.1.1-3 Geological Route Map
(4) PL II.1.1-4 Location Map of Rock Samples
(5) PL II.1.1-5 Detailed Sketch of Geothermal Manifestation
(6) PL II.1.1-6 Zonal Distribution of Alteration Zone

(7) PL II.1.2-1 Bouguer Anomaly
(8) PL II.1.2-2 Gravity Trend
(9) PL II.1.2-3 Residual Gravity
(10) PL II.1.2-4 Deep Gravimetric Component (1,200 m)
(11) PL II.1.2-5 Shallow Gravimetric Component (190 m)
(12) PL II.1.2-6 Underground Structure (Profile A-A')
(13) PL II.1.2-7 Underground Structure (Profile B-B')
(14) PL II.1.2-8 Underground Structure Profile (C-C')
(15) PL II.1.2-9 Underground Structure (Horizontal Section)

(16) PL II.1.3-1 Total Magnetic Intensity
(17) PL II.1.3-2 Total Magnetic Anomaly
(18) PL II.1.3-3 Upward Continuation
(19) PL II.1.3-4 Deep Magnetic Component
(20) PL II.1.3-5 Shallow Magnetic Component
(21) PL II.1.3-6 Result of Magnetic Modelling
(22) PL II.1.3-7 Underground Magnetic Structure

(23) PL II.2.1-1 Apparent Resistivity Isocontours (T=0.11 sec)
(24) PL II.2.1-2 Apparent Resistivity Isocontours (T=1.1 sec)
(25) PL II.2.1-3 Apparent Resistivity Isocontours (T=39 sec)
(26) PL II.2.1-4 Total Conductance
(27) PL II.2.1-5 Structure Isocontours for the Top of the Shallow Conductive Formation
(28) PL II.2.1-6 Structure Isocontours for the Top of the Deep Conductive Formation
(29) PL II.2.1-7 Isopachs of the Overburden overlying the Deep Conductive Formation
(30) PL II.2.1-8 Top of Electric Basement
(31) PL II.2.1-9 Subset Map
(32) PL II.2.1-10 Locations of Cross Section

(33) PL II.2.2-1 Seismic Survey Line Map
(34) PL II.2.2-2 Refraction Method Analysis Map
(35) PL II.2.2-3 Weathering Layer Velocity Distribution Map
(36) PL II.2.2-4~8 Side Reflection Analysis Map
(37) PL II.2.2-9 Side Reflection Distribution Map
(38) PL II.2.2-10~14 Diffraction Source Distribution Map
(39) PL II.2.2-15 Temperature Distribution Map of Holes (Depth 10 m)
(40) PL II.2.2-16~20 Final Stack (Time Section)
(41) PL II.2.2-21~25 Amplitude Distribution Map
(42) PL II.2.1-26~30 Frequency Distribution Map
(43) PL II.2.2-31~35 Time Section Map (with Reflective Layer)
(44) PL II.2.2-36~40 Final Stack (Depth Section)
(45) PL II.2.2-41~43 Depth Section Map
(46) PL II.2.2-44 Structure Analysis Map (L_1)
(47) PL II.2.2-45 Structure Analysis Map (L_2)
(48) PL II.2.2-46 Structure Analysis Map (DL-1,000 m)
(49) PL II.2.2-47 Structure Analysis Map (DL-2,000 m)

(50) PL III.2-1 Compiled Column (GTF-1)
(51) PL III.2-2 Compiled Column (GTF-2)
(52) PL III.2-3 Compiled Column (GTE-3)
(53) PL III.2-4 Compiled Column (GTE-4)
(54) PL III.2-5 Compiled Column (GTE-5)

(55) PL IV-1 Factor Score Map for Regional Model (Factor 1)
(56) PL IV-2 Factor Score Map for Regional Model (Factor 2)
(57) PL IV-3 Factor Score Map for Regional Model (Factor 3)

No. 39

THE PRE-FEASIBILITY STUDY FOR THE SAN KAMPAENG GEOTHERMAL DEVELOPMENT PROJECT IN THE KINGDOM OF THAILAND

TECHNICAL REPORT

(THE 1st AND 2nd PHASE STUDY)

JANUARY, 1984

JAPAN INTERNATIONAL COOPERATION AGENCY

THE PRE-FEASIBILITY STUDY
FOR
THE SAN KAMPAENG GEOTHERMAL DEVELOPMENT PROJECT IN THE KINGDOM OF THAILAND

TECHNICAL REPORT

(THE 1st AND 2nd PHASE STUDY)

JANUARY, 1984

JAPAN INTERNATIONAL COOPERATION AGENCY

PREFACE

This report has been written for the presentation of the results of "The Pre-Feasibility Study on the San Kampaeng Geothermal Development Project in the Kingdom of Thailand", conducted by the Japan International Cooperation Agency. The surveys were carried out to evaluate the possibility of geothermal development in the San Kampaeng area in the Kingdom of Thailand. The surveys are composed of the primary investigation of geological survey, gravity survey and magnetic survey, and of the secondary investigation of deep electric survey and seimic survey. Technical guidances on the methods of the well logging were held twice in the period of these investigations for the technical staffs of the Thailand.

The actual survey works were performed with the cooperation of the Thailand side counterpart, comprising Electricity Generating Authority of Thailand: EGAT, Department of Mineral Resources: DMR and Chiang Mai University: CMU. They are greatly acknowledged. Many informations and data, which had been obtained through the geothermal investigations conducted by the Thailand side were supplied for this survey. These informations were of great help to the synthesized analysis of the survey results.

CONTENTS

TABLE FOR MAPS

1 INTRODUCTION

I INTRODUCTION

I-1 Purpose of the Survey

This pre-feasibility study was performed so as to clarify features of geothermal distribution in the San Kampaeng area, and to evaluate possibilities of geothermal development in the area. The study was executed by the Japan International Cooperation Agency. For the purpose of the study, geological survey, gravity survey, magnetic survey, well logging of the model test wells and technical guidance were carried out as the primary investigation, and deep electric survey, seismic survey and collection of the data of the exploration wells were completed as the secondary investigation.

The results of the primary investigation were presented in the "Interim Report" published in 1982.

In the present report, are contained the survey results and analysis results of the primary and the secondary investigations, in addition to the synthesized consideration on them.

I-2 Surveyed Area

The San Kampaeng geothermal area is located about 30 km east of city of Chiang Mai, in the state of Chiang Mai, in the northern part of the Kingdom of Thailand. The area is situated in the range of latitudes between 18°45′, and 18°50′ and of longitudes between 99°13′ and 99°17′, and the area is about 50 square kilometers (Fig. I-1).

The area where the geothermal indications are found is in the middle of Wat Pong Hom and Ban Pong Nok in the northwestern part of the surveyed area, and is characterized by the distribution of many hot springs with high temperature.

In the west of the surveyed area, the Doi Luang mountaneous land runs in north and south at the altitude of 500 to 650 meters above sea level, while in the east of it, the Mae Tha mountaneous land is seen to extend in north and south at the altitude of 500 to 850 meters above sea level. Flat lowland occupies the area between them, with the width of several kilometers and at the altitude of 350 to 450 meters above sea level.

I-3 Term of the Survey

The primary investigation, which is composed of geological survey, gravity survey, magnetic survey, well logging of the model test wells and technical guidance, started in the field on 6th of July, 1982, and finished on 28th of December, 1982, following the schedule in the program. As for the logging of the test wells and the technical guidance, the program was changed following the schedule of drilling of the exploration wells by the Thailand side, – that is, advancing the programmed date of 15th of March, 1983 by about two months, the works began on 23rd of January, 1983. Also, the term of the works was reduced to 10 days while 20 days had been prepared in the original program.

The secondary investigation, which is composed of deep electric survey, seismic survey and collection of the data of the exploration wells, was completed on 24th of June, 1983, as had been programmed.

The term of the survey is shown in the Table I-1.

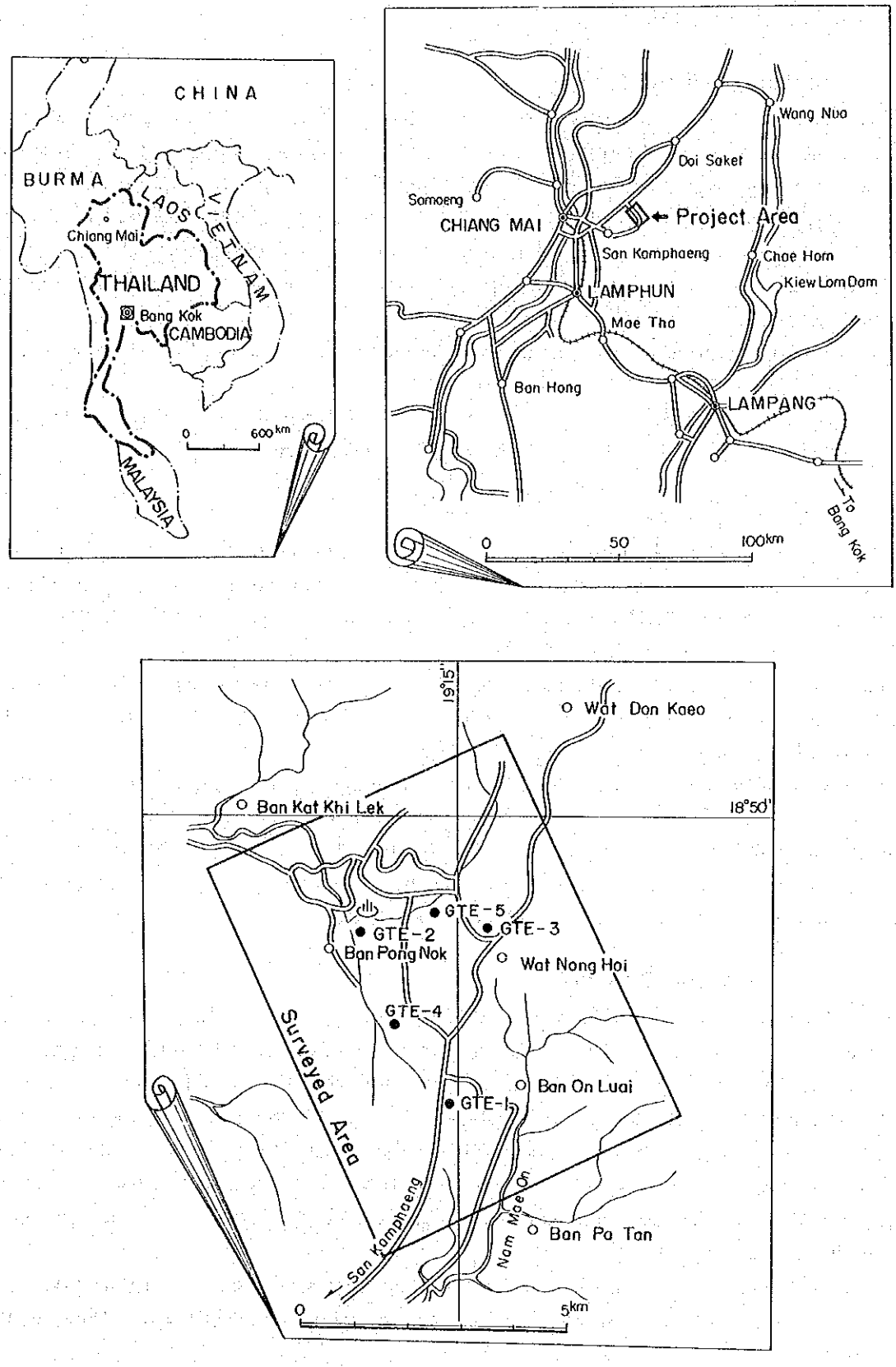

Fig. I-1 Location of project area

Table I-1 Term of the survey

Item \ Term		Field Survey	Analysis
Primary Investigation	Geological survey	From July 6, 1982 to Aug. 5, 1982 31 days	From Aug. 6, 1982 to Mar. 31, 1983
	Gravity survey	From Nov. 1, 1982 to Dec. 28, 1982 58 days	From Jan. 4, 1983 to Mar. 31, 1983
	Magnetic survey	From Nov. 1, 1982 to Dec. 28, 1982 58 days	From Jan. 4, 1983 to Mar. 31, 1983
	Logging of exploration well and technical guidance	(First) From July 28, 1982 to Aug. 16, 1982 20 days (Second) From Jan. 23, 1983 to Feb. 1, 1983 10 days	
Secondary Investigation	Deep electric survey	From Jan. 4, 1983 to Feb. 22, 1983 50 days	From June 1, 1983 to July 30, 1983
	Seismic survey	From Jan. 4, 1983 to Mar. 31, 1983 87 days	From Apr. 1, 1983 to Sep. 8, 1983
	Collection of the data of exploration wells	From June 15, 1983 to June 24, 1983 10 days	

I-4 Members of the Survey Team

The leaders and the members of the respective survey teams are listed in the following (Table I-2).

Table I-2 List of the members of the survey team

Survey	Name of Member		Position
Leader	Nakamura	Hisayoshi	J.M.C.
Geological survey	Wakabashi	Kensuke(*)	MINDECO
	Tagami	Yukhichi	MINDECO
	Ide	Toshio	J.M.C.
Gravity survey	Kimura	Mikio(*)	MINDECO
Magnetic survey	Miyoshi	Fukujiroh(*)	MINDECO
Logging of exploration wells and technical guidance	Takayama	Takao(*)	Kaihatsu Kogyo Co., Ltd.
	Obara	Yukimasa	J.M.C.
Deep electric survey	Nobuchi	Kazuhisa(*)	J.M.C.
	Takasugi	Shinji	J.M.C.
Seismic survey	Aribe	Akira(*)	Ube Industries Co., Ltd.
	Nohara	Kazuyoshi	Ube Industries Co., Ltd.
	Kawamura	Kohji	Ube Industries Co., Ltd.
	Suzukawa	Toshimichi	Ube Industries Co., Ltd.
	Hori	Takashi	Ube Industries Co., Ltd.
Collection of the data of exploration wells	Wakabayashi	Kensuke(*)	MINDECO

(*) Leader of the respective survey team

MINDECO : Mitsui Mineral Development Engineering Co., Ltd.
J.M.C. : Japan Metals and Chemicals Co., Ltd.

Table I-3 List of members of Thailand-side counterpart

Survey	Name of member		Position
General affairs	CHAYA	JIYACAT	EGAT
	CHAI	ASA BHOTIRUNGSIYAKORN	EGAT
	KIATICHAI	PATIKONSIN	EGAT
	AMNUAYCHAI	TIENPRASERT	DMR
Geological survey	SURACHAI	PRASERDVIGAI	EGAT
	VISIT	COOTHONGKUL	EGAT
	ADICHAT	SURINKUM	DMR
	PRAPAT	SOPHONPONQPHIPAT	DMR
Gravity survey	SURACHAI	PRASERDVIGAI	EGAT
	VISIT	COOTHONGKUL	EGAT
	PRECHA	LAOCHU	DMR
Magnetic survey	SURACHAI	PRASERDVIGAI	EGAT
	PAIROAG	RANGPOLSUMRIT	DMR
Logging of exploration wells and technical guidance	JIRAKOM	PADUMANON	EGAT
	BUNCHA	KONGSUPAKPUL	EGAT
	EKACHI	SINRATAPAKDI	EGAT
	PRAMUAL	WONGPUNGA	EGAT
	SOMMART	SARI	EGAT
Deep electric survey	SURACHAI	PRASERDVIGAI	EGAT
	WANCHAI	PRASARTKETVITAYA	EGAT
	SUEBSAK	SOLGOSOOM	DMR
Seismic survey	SOMCHAI	WONGPORNPAXDEE	EGAT
	SURACHAI	PRASERDVIGAI	EGAT
	SUTHEP	LERTSRIMONGKOL	EGAT
	VISIT	COOTHONGKUL	EGAT
	PRECHA	LAOCHU	DMR

EGAT : Electricity Generating Authority of Thailand
DMR : Department of Mineral Resources

I-5 Content of the Survey

Content and amount of the respective survey are shown in the following table (Table I-4).

Table I-4 Contents of the survey

Survey	Amount	Contents
Geological survey	Total length of surveyed routes is 95 km approx. Thin sections: 55 Fossil determination: 5 Age determination: 5 Analysis by X-ray diffraction: 103	Stratigraphy: Divided into Carboniferous Mae Tha Formation (lowest), Permian Kiu Lom Formation, Triassic granite and alluvium (upper-most) Fault system: Main fault system has NNW-SSE trend Other trends such as NNE-SSW NW-SE and NE-SW are recognized. Alteration: Developed around the area where the geothermal indications are distributed, and is divided into 5 zones.
Gravity survey	Survey points: 230 Compiled points: 87 Samples for measurement of rock density: 84	Iso-gravity contours have trends of N-S, NW-SE and NE-SW dominantly. The middle to upper part of the Kiu Lom Formation corresponds to high gravity anomaly while the lower part of it corresponds to low gravity anomaly. The area where the geothermal indications are distributed is corresponding to low gravity anomaly.
Magnetic survey	Survey points: 901 Measurement of magnetic susceptibility: 84 Field measurement of magnetic susceptibility: 9 localities	Magnetic bodies (magnetic anomalies) are expected in the south of the Ban Mae Khu Ha fault, along the Hual Mae Khu Ha fault and along the Huai Wai fault
Logging of the exploration wells and technical guidance	Logged wells: GTE-3 GTE-4	Truck-mounted geophysical logging system and apparatus (temperature, pressure, resistivity, s.p., caliper, sonic and flow rate) were used for logging works. The hole GTE-3 was logged to the depth of 88 m, while the hole GTE-4 was logged to the depth of 164 m.
Deep electric survey	Survey points: 33	Total conductance value is low as a whole. Geothermal indication zone and southeastern part of the surveyed area (around Wat Hua Fai) are revealing high values of conductance of more than 300 mhos.
Seismic survey	Survey lines: 5 Total length of survey lines: 14,225 m Shot holes: 315	From the stacking records of reflection survey, supposed horizons of L_1~L_8 are recognized. It is inferred that the shallower part than the horizon L_8 is Paleozoic formations, while the deeper part is granite. From the tendency of distribution of the diffraction sources, 6 faults of NW-SE trend, 4 faults of N-S trend and a fault of E-W trend are estimated.
Collection of the data of exploration wells	Subject wells: 5 holes	Informations of geologic survey and well logging data were collected on the five exploration wells of GTE-1 to GTE-5, drilled by EGAT.

II SURVEYS CONDUCTED BY JAPAN INTERNATIONAL COOPERATION AGENCY

II SURVEYS CONDUCTED BY JAPAN INTERNATIONAL COOPERATION AGENCY

II-1 Primary Investigation

II-1-1 Geological Survey

1. Foreword

The geological survey was carried out for the purpose to estimate structural conditions of the geothermal reservoirs in the San Kampaeng area, by clarifying lithofacies, stratigraphy, geological ages and geological structures of the formations underlying this area and by elucidating relation of the geology to the geothermal features (geothermal indications, distribution of alteration zones, etc.) or to the other survey results obtained.

For the geological survey, was used the topographical map of the scale of 1 to 10,000, which had been prepared by enlarging the map of the scale of 1 to 50,000 published by the government of the Kingdom of Thailand. Along the main routes, geological mapping and alteration surveys were carried out. Also, in the significant areas like the area where the geothermal indications are distributed, detailed mapping was carried out, after large scaled map was drawn through simplified land surveys. The rock samples collected in the surveys were brought back to Japan, where they were supplied to microscopic observation, to fossil determination, to age determination and to X-ray diffraction analysis, according to the subject of the samples.

2. Field works

The geological survey was completed in approximate area of 50 km^2 and along the selected routes of the total length of 95 km. The topographical map used for the mapping was, as mentioned above, the enlarged map of the scale of 1 to 10,000, but as actual land features were not always in good correspondence to the map, simplified land surveys by small transit compasses and plastic measuring tapes were employed to draw up route maps in the scale of 1 to 5,000, for the geological mapping.

As for alteration surveys, route maps of the scale of 1 to 2,000 were made up in the area from Ban Pong Nok to Wat Pong Hom, where the geothermal indications are distributed remarkably. Hydrothermal alteration was rarely recognized in the other area than the abovementioned geothermally indicated arcas.

3. Method of Analysis

The materials collected in the field surveys were supplied to laboratory examination, that is, to microscopic observation, to fossil determination, to age determination and to X-ray diffraction analysis.

Microscopic observation: Thin sections of the representative 51 rock samples were prepared and supplied to the observation under microscope for the identification of minerals and for the determination of rock species.

Fossil determination: Five samples of limestone, in which fossils of foraminifera and so on had been recognized in the field, were supplied to fossil determination for the geological ages.

Age determination: Five samples were collected of the igneous rocks (basalt and granite)

distributed in the survey area, and supplied to age determination by K-Ar method.

X-ray diffraction analysis: Alteration minerals were identified by the X-ray diffraction analysis of the 103 samples of the altered rocks collected in the area where the geothermal indications are distributed.

According to the results of the fieldworks and the laboratory examination as mentioned above, the geological map, the geological profiles and the zonal distribution map of alteration zones were drawn up, and by these maps, lithofacies, stratigraphy, geological ages and geological structure of the formations underlying the surveyed area were clarified in addition to the comprehension of the relation between the geological structure and the geothermal indications or the distribution of the alteration zones.

4. Survey results

4-1 Geological Environment in and around the surveyed Area

Outline of the geological environment in and around the surveyed area is presented here to help the comprehension of the geology of the San Kampaeng geothermal area (Fig. II.1.1-1). The northern part of the Kingdom of Thailand, including the surveyed area, is located almost in the middle of the Indosinian peninsula.

The oldest rocks (basement) in the Indonesian penninsula are the metamorphic rocks (gneisses, Paleozoic granites) formed in the period of the orogeny at the end of Pre-Cambrian age or in the earliest Paleozoic Era. They are distributed in the Kontum plateau in the southern part of Vietnam, close to the border to Cambodia, and in the basin of the Hong River in the northern part of the Republic of Vietnam. They are also distributed in and around Myitkyina in the northern part of Burma, and in the area west of Chiang Mai in the northern part of the Kingdom of Thailand. These metamorphic rocks compose the cratonized cores of oldest continents.

Around these continent cores, are distributed, in order, the orogenic zones of the periods of Hercynian (Carboniferous), Indosinian (mainly Triassic, though from Permian to Jurassic) and Himalayan (Cretaceous to Quaternary). It is thought that the younger formations were added to these continent cores with the change of the times, which would have brought about the development and the enlargement of the cores.

The Hercynican orogenic zone is distributed in the eastern part of the Indosinian peninsula, and composes the Annatomian massif.

The Indosinian orogenic zone is distributed all over the Indosinian peninsula, and composes the Indosinian massif.

The Himalayan orogenic zone is found to extend from Burma, through the Andaman Sea, to Sumatra island and Java island. Borneo and Philippine islands are also included in this Himalayan orogenic zone, and the distribution of this orogenic zone is found surrounding the Indosinian massif. The Himalayan orogenic activity had some effect to the Indosinian massif, such as gentle undulation and fault block movement. It is thought that these movements would have constituted important factors to divide land and shelf of the Indosinian massif, and that these movements resulted in the formation of the folding structures with axes of two different directions of E-W or WNW-ESE and N-S or NNE-SSW.

The geological structure recognized in the Kingdom of Thailand at present is thought to be the products of multi-orogenic movements, affected especially by block movement associated

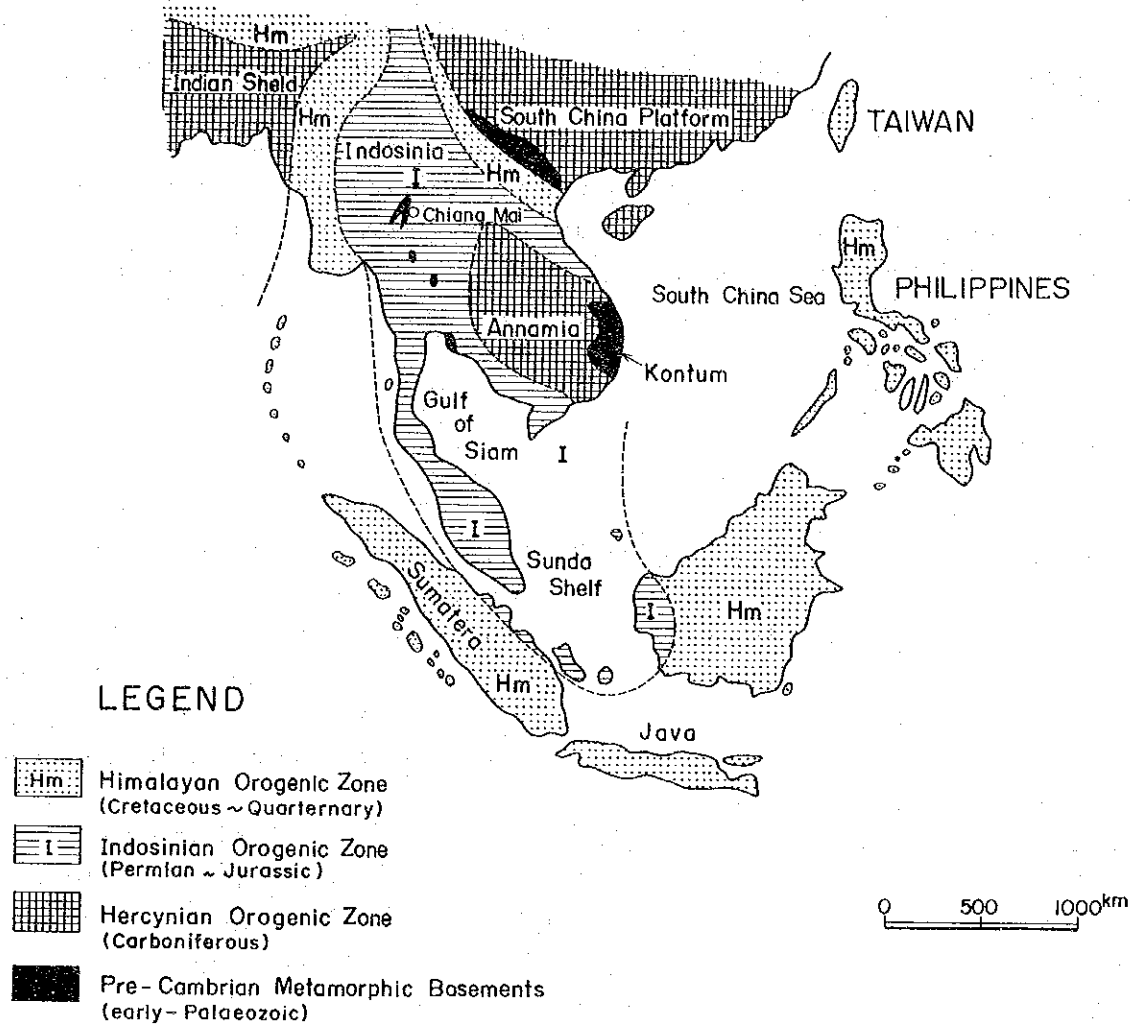

Fig. II.1.1-1 Major geological unit of southeast Asia

with the orogenic movement. The block movement has continued until the present age since the Tertiary Period and has given some influences against the geological structure of the upper Tertiary system as well as against the forms of Quaternary terraces. The causes of the block movement continuing up to the present age are thought to be the expansion of the Andaman Sea and accompanying development of tension zone from the northern part of the Kingdom of Thailand to Burma. The hipocenters of the earthquakes in the Burmese area have tendency to be plotted the deeper, the more eastward. The distribution of the epicenters of these earthquakes is along the extension of the Java trough, which is located outside the Indonesian islands. From these facts, it is thought that the geological structure in the area from Burma to the northern part of the Kingdom of Thailand has almost same characteristics as that of island arcs.

The northern part of the Kingdom of Thailand is divided into the following four tectonic provinces composed of different geological structure formed according to the results of the block movement (Fig. II.1.1-2).

1) West Tectonic Province
2) Main Western Range Tectonic Province
3) Central North Tectonic Province
4) East Tectonic Province

The West Tectonic Province occupies the westernmost part of the Kingdom of Thailand, west of Mae Sariang and Mae Sot. The formations underlying this area are composed of thick layers of carbonate rocks and clastic sediments of Carboniferous to Jurassic system. No volcanic rock has been recognized. The area composes subsided zone by fault movement, covered with Quaternary freshwater sediments, about 300 meters thick. This province extends to the west, crossing the border to Burma, where it corresponds to the peripheral zone of the trough west of the Shan-Thai massif.

The Main Western Range Tectonic Province includes main mountaneous land of the Kingdom of Thailand, between Mae Sariang and Chiang Mai, and extends southward as far as to Kanchanaburi. The province is underlain geologically by the Pre-Cambrian metamorphosed sedimentary rocks accompanying arch-like intrusive body of granite and weakly metamorphosed early Paleozoic shelf sediments overlying the former uncomformably. The Pre-Cambrian metamorphic rocks in this province are distributed separately from the Kontum massif in the Indosinian peninsula, and belongs to what is called to be Shan-Thai massif. This province is characterized, as whole, to be uplifted massif by fault movement.

The Central North Tectonic Province occupies the area extending widely in north and south in the central part of the Kingdom of Thailand. The extension of the province is from Chiang Rai in the north to Chanthaburi, through Uttaradit. The rocks underlying the province are composed of sedimentary rocks of the facies of continental margin and calc-alkaline volcanic rocks of the periods of middle Paleozoic to early Mesozoic. This province is characterized by the intense folding structure and thrust faults. It is thought that the above structural characteristics would have been formed by the subsidence of the eastern massif toward the west from the eastside, in the period of late Paleozoic to early Mesozoic era. That is, during the period of this subsidence, eruption of basic volcanic rocks occurred actively along the eastern marginal zone of the Shan-Thai massif. These volcanic rocks and clastic sediments from the eastern massif were supplied to the sedimentary basin in the east of the Shan-Thai massif, to form thick sedimentary formations. The formations were folded and faulted remarkably by the later orogenic movement.

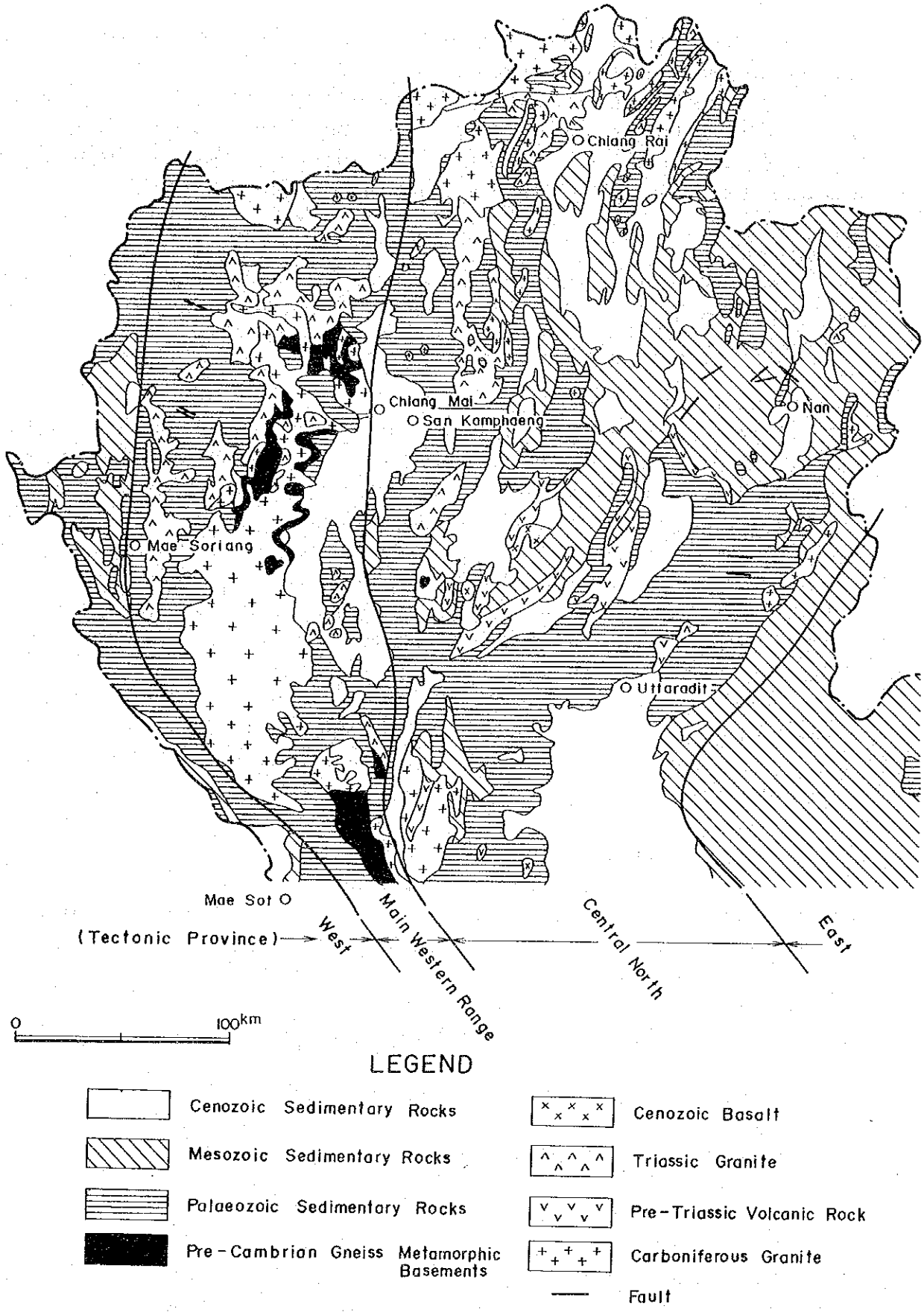

Fig. II.1.1-2 General geology of northern Thailand

Intrusion of Cenozoic basalt is recognized partly. The San Kampaeng geothermal area is situated in the western peripheral zone in the northern part of this province.

The East Tectonic Province is represented by the Khorat plateau area in the northeastern part of the Kingdom of Thailand. The formations underlying this province are composed of thick red layers, including evaporites, of late Triassic to Cretaceous periods. They are thought to be continental shelf sediments. The folding is comparatively weak in this province.

4-2 Stratigraphy

The rocks underlying the surveyed area are composed, from the lowest, of Carboniferous Mae Tha Formation, middle Permian Kiu Lom Formation in the Ratoburi Group, Triassic granites and alluvium deposits (Fig. II.1.1-3).

4-2-1 Mae Tha Formation

The layers of this formation are distributed in the western mountaneous land as well as in the east of the eastern mountaneous land. They are composed mainly of compact, hard, white-colored massive medium grained sandstone, although insertions of thin dark-colored shale are recognized in the eastern part. Quartz veinlets are developed in this formation. Under microscope, the rocks are composed mainly of round or sub-round sand grains, 0.1 – 10 mm in diameter, of quartz and sericitized feldspar, though large grains over 1.0 mm in diameter are contained in some occasion. The matrix filling the space is mainly recrystallized quartz, with sericite and clay minerals. Limonite-quartz veinlets are well developed and muscovite, biotite, zircon and sphene are also recognized.

This formation forms the basement in this surveyed area, and as it is in contact with the Kiu Lom Formation by fault, actual stratigraphical relation of these formations is uncertain. The thickness of this formation is estimated to be more than 1,600 meters, although the upper and the lower limit are not confirmed.

4-2-2 Kiu Lom Formation

The layers of the Kiu Lom Formation are distributed widely in an area extending in NNW-SSE direction, occupying the central zone of the surveyed area. The formation is divided into three units from the lithofacies; the lower part of sedimentary rocks, the middle part of limestone and the upper part of volcanic rocks.

(1) Lower part of the Kiu Lom Formation

The lower part of the Kiu Lom Formation is divided, from the lowest upward, into the following.

Alternation of limestone and shale
Sandstone bed
Alternation of siltstone, sandstone and chert
Chert bed
Alternation of siltstone and sandstone
Sandstone bed

Alternation of limestone and shale is composed mainly of light grey to dark grey limestone and black shale, with grey sandstone layers. They are distributed dominantly in the east of Ban On Luai, and are confirmed by the drill hole GTE-2. The limestone of this alternation contains

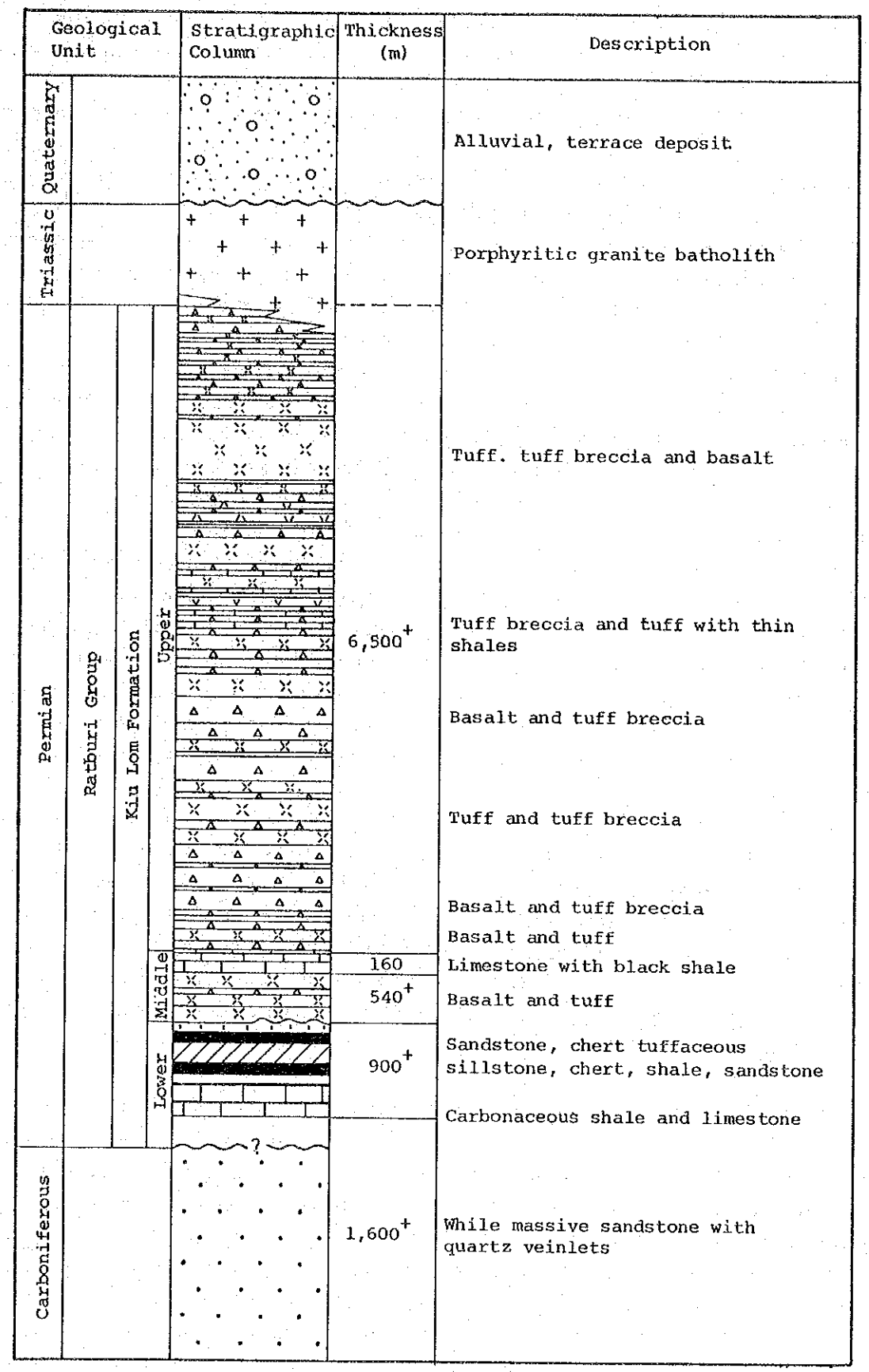

Fig. II.1.1-3 Geological column of project area

foraminifera fossils of Neoschwagerina, Sumatrina etc. (Table II.1.1-1), and its age is thought to be middle Permian. This alternation is situated at the lowest of the Kiu Lom Formation, but as the lowest limit of this alternation has not been confirmed, the relation of this alternation to the Carboniferous Mae Tha Formation is uncertain. The thickness of this alternation is more than 600 meters.

Sandstone bed is represented by the white medium grained sandstone exposed in the hilly land in the northwest of Wat Pong Hom. It is massive and unstratified. Under microscope, the rock is composed of hardly-sorted and sub-angular sand grains of fine to coarse grained quartz, kali-feldspar and plagioclase. The matrix is composed of sericite and clay minerals. Small amount of well-rounded grains of biotite, muscovite, zircon, leucoxene, tourmaline and quartzite are recognized. The thickness of this sandstone bed is about 60 meters.

Alternation of siltstone, sandstone and chert is distributed in the area from Ban Pong Hom to Huai Ang River, in the western part of the surveyed area and from Nam Mae On to Nam Mae Lai in the eastern part. This alternation is composed mainly of siltstone inserted with sandstone and chert. The siltstone is well-stratified and dark grey, but it looks white when hydrothermally altered. Under microscope, the siltstone is composed mainly of sub-angular grains, 0.03 to 0.1 mm in diameter, of quartz and plagioclase. Schistose structure and cleavages in two directions are recognized. As a whole, limonite contamination is remarkable. When altered, this siltstone becomes white and soft, and microscopically are recognized microcrystalline or cryptocrystalline quarts, sericite, kaoline, anatase and alunite, etc. Sandstone is dark grey. Under microscope, it is composed of sub-angular or sub-rounded, well-sorted minute grains of quartz, kali-feldspar and plagioclase, and consolidated with the matrix of sericite and clay minerals. Small amounts of sphene, muscovite, zircon and quartzite are also recognized. Chert is white to milky white in color, composing inserted layers as thin as 1.0 – 3.0 cm in the siltstone. The thickness of this bed is about 200 meters.

Chert bed is distributed in the area from Ban Pong Hom to the east of the Huai Ang River. This bed is composed mostly of chert, but insertions of siltstone are observed in the lower part while the layers of sandstone and siltstone are inserted in the upper part of this bed. Chert is compact, white or milky white in color, with resinous luster. It is often fractured into small pieces. Under microscope, microcrystalline and cryptocrystalline quartz, chalcedony and opal are recognized, in mozaic texture, with sericite, limonite and micrograins of opaque minerals. Also, some spherical or needle-like crusts replaced by chalcedonic quartz are observed microscopically. It is thought that they are fossils of radioralia replaced by quartz. The thickness of this bed is about 200 meters.

Alternation of siltstone and sandstone is distributed in the area from Ban Pong Hom to the Huai Ang River. This alternation is composed mainly of siltstone with insertions of sandstone layers. The siltstone is argillized and light grey or milky white in color. In many cases it is weathered. Under microscope, it is muddy rock containing well-sorted quartz grains. It is composed of micrograins of quartz, sericite, clay minerals and limonite. The sandstone layers inserted in the siltstone are greyish white and compact, forming alternation of the approximate thickness of every 1 meter. This alternation is roughly as thick as 150 meters.

The sandstone bed is distributed in the area from the east of Ban Pong Nok. The composing rock of this sandstone bed is massive hard and white, medium-grained sandstone. The thickness

Table II.1.1-1 Identification of fossils

Sample Number	T - 099	E - 051	E - 055	W - 011	W - 015
Rock Name	Limestone	Limestone Breccia	Limestone	Limestone breccia	Limestone
Locality	X = 29,670 E Y = 77,280 N	X = 25,310 E Y = 76,940 N	X = 25,510 E Y = 77,630 N	X = 25,930 Y = 80 780	X = 25 720 E Y = 79,680 N
Age	Middle Permian	Carboniferous	No Determined	No Determined	Middle ? Permian
Fossils	Fusulinid Neoschwagerina Sumatrina Parafusulina ? Chusenella ? Crinoid Stem: Algae:	Fusulinid: Profusulinella ?? Coral flakes Bryozoa Algae ?	Crinoid Stem	Algae ?	Fusulinid: Schubertella Sp ? Kahlerina Crinoid stem Endothyrida Algae
Remark	Neoschwagerina and Sumatrina indicate that the strata is middle-Permian in age. Most of fusulinid are deformed and partly broken.	This strata is not exactly determined in age, because Fusulinids are rate and imperfect. They are asumed as Profusulinella of middle Carboniferous age for their size and shell structure. However, it is doubtful in age because an axial plane is not dtestable.	This rock is highly recrystallized. Geological age is impossible to determine because of only crinoid stems.	Rock facias is resemble to E-051 No age-determinable fossils are detected and no fossils in colitic limestone pebble are recognized.	Schubertella is found in early – middle Permian formation and Kahlerina is observed in middle Permian formation It shows most possibility that the strata is middle Permian in age.

of the bed is about 150 meters.

(2) The middle part of the Kiu Lom Formation

The middle part of this formation is divided into two units: the lower layers of basaltic lava and tuff and the upper layers of limestone and shale.

The basaltic lava and tuff, the lower layers, are distributed around Ban Mae Khu Ha and in its northern and southern area. The basaltic lavas are found seated with the thickness of 5 to 10 meters in the basaltic tuffs. The lavas are dark to deep green, vesicular and massive. Under microscope, it has porphyritic texture with the phenocrysts of saussuritized plagioclase, about 1.0 mm in diameter, and opacitized pyroxene, about 0.5 mm in diameter, recognized in the fine grained basaltic matrix. Chlorite, epidote and pumpellyite are recognized as alteration minerals. The basaltic tuffs are pale to deep green in color, forming lapilli tuff and tuff breccia in some parts. The basaltic tuff changes its lithofacies to the black shale gradually in the uppermost part, with bedding planes well-developed. The thickness of the basaltic lava and tuff is about 540 meters.

The limestone and the shale, the upper layers, are distributed along the small hilly land forming character of "S" in north and south, in the central part of the surveyed area. The limestone is black to grey in color, and accompanies layers of black phyllitic shale of the thickness of 10 to 20 meters in its hanging and footwall sides. This limestone is massive in many places, although layers of thin shale are inserted in some places. It is recrystallized limestone, containing many fossils of fusulina, coral, bryozoan and algae, which are not well preserved. Although there are few fossils by which age of the bed can be determined, it is possible to take the age to be middle Permian viewing from the existence of Schubertella sp. and Kahleria (Table II.1.1-1). The shale is calcareous where it lies next to limestone, while it is tuffaceous where it is in contact with tuff. The shale is phyllitic and fissility developes in it. Under microscope, the calcareous shale is composed of sandy or silty grains of quartz and calcite in the matrix of chlorite, sericite and calcareous materials. The tuffaceous shale is composed mainly of schistose quartz and sericite, in the microcrystalline matrix of plagioclase, sphene and limonite. The thickness of this limestone and shale is about 250 meters.

(3) Upper part of the Kiu Lom Formation

The upper part of the Kiu Lom Formation is composed of basaltic lava, tuff, lapilli tuff and tuff breccia, partly inserted with thin layers of tuffaceous sandstone, chert and siltstone. This upper part of the Kiu Lom Formation is distributed widely in the central part of the surveyed area, but its structural features had not been known clearly. By the result of the detailed mapping in this geological survey, which was carried out in a way to trace each layers following the division of lithofacies as above-mentioned, it has been clarified that the geological structure of this upper part of the formation is similar to that of the middle part and of the lower part of the formation. The basaltic lava is several to 20 meters thick and its continuation is comparatively well. The lava is deep to dark green in color, vesicular and massive. Under microscope, porphyritic texture is observed in many cases, although it shows glomeroporphyritic or autobrecciated texture in some cases. Phenocrysts are clinopyroxene and plagioclase. The plagioclase is often saussuritized. The matrix is composed of plagioclase and clinopyroxene exhibiting ophitic texture, associated with chlorite, epidote, zeolite and pumpellyite formed by alteration.

By the results of the age determination of this lava by K-Ar method, values of the ages are pretty scattering, as 389 ± 19 m.y., 206 ± 10 m.y., 190 ± 10 m.y. and 119 ± 14 m.y. (Table II.1.1-2). It is thought to be possible as the reasons for the values to be scattering so much, that the differences with the amount of elements for age determination would have been produced by the geological environment at the period of the effusion of the lavas as well as through the alteration after flowing out. Especially in case of oceanic basalt, excessive Ar is easily produced as ^{40}Ar by rapid cooling and pressure, which it is known, would render the values of the K-Ar age to be older apparently. Also, it is said that alteration can reduce the values of K-Ar ages to be younger, by Ar-loss and K-addition. The environment of the effusion of the subject lava is thought mostly to be in shallow sea, though partly on land, viewing from the fact that it alternates with shale, sandstone and limestone. Also, such alteration minerals as chlorite and pumpellyite have been produced in the lava by the alteration. Meanwhile, by fossil data the period of the sedimentation of the Kiu Lom Formation is shown to be middle Permian, which does not correspond to the results of the age determination by K-Ar method. Accordingly, it is thought that the values obtained by the age determination by K-Ar method do not reveal appropriate ages of formation of this lava. Probably this was brought about by the environment of the sedimentation at the period of the effusion and by the alteration with intrusion of granite at the period of latest Triassic.

Table II.1.1-2 K-Ar age determination of igneous rocks

Sample Number	Rock Name	Locality	Mineral	Age (m.y.)	Ar^{40} Rad SCC/gm $\times 10^{-5}$	Ar^{40} Rad%	K %
W-006	Basaltic Welded tuff	Wat Don Kaeo	Whole Rock	119 ± 14	0.024 0.024	12.7 20.8	0.05 0.05
W-009	Pyroxene Basalt	Wat Nong Hoi	Whole Rock	389 ± 19	0.067 0.068	42.3 36.9	0.04 0.04
W-017	Pyroxene Basalt (Altered)	Huai Hat	Whole Rock	206 ± 10	0.836 0.852	89.7 91.2	0.99 1.00
T-103	Biotite Granite	Ban Huai Kaeo	Biotite	212 ± 10	2.84 2.90	81.2 86.6	3.27 3.31
T-107	Pyroxene Basalt	Ban Mae Koha	Whole Rock	190 ± 10	0.751 0.751	88.4 90.1	0.96 0.97

The constants for the age calculations are: $\lambda_\beta = 4.96 \times 10^{-10} yr^{-1}$,
$\lambda = 0.581 \times 10^{-10} yr^{-1}$, $^{40}K = 1.167 \times 10^{-4}$ atom per atom of natural potassium.

The basaltic tuff, lapilli tuff and tuff breccia are observed to form alternation in the thickness of several meters or several ten meters, and the lateral continuation is comparatively well. Under microscope, the basaltic tuff is composed of pieces of basalt of the diameter of 0.8 to 2.5 mm, and of crystal pieces of pyroxene and plagioclase with glass pieces, in the matrix of fine grained chlorite, quartz, plagioclase, epidote, pumpellyite, sericite and zeolite. The lapilli tuff and the tuff breccia are composed of breccias of various hollocrystalline to glassy basalts with the basaltic tuffaceous matrix.

The tuffaceous sandstone is distributed around Ban On Klang. It is dark green, and it forms alternation of fine grain layers and coarse grain layers in the thickness of 2 to 5 cm. Under microscope, this tuffaceous sandstone is composed of alternation of coarse grained lithic wacke and fine grained feldspathic wacke which were thought to have originated from basaltic clastic rocks. The grains are angular to sub-angular. Clay minerals, sericite and limonite are recognized.

The chert is distributed around Ban Mai Takhian. It is dark grey, hard, compact and well-stratified rock. Along the margin in contact with tuff, this chert becomes dark green and coarse grained.

The tuffaceous sandstone, chert and siltstone are found as thin layers, as thick as less than several ten meters, in the basaltic tuff.

The total thickness of the upper part of the Kiu Lom Formation is estimated to be more than 6,500 meters.

4-2-3 Granites

The granites are distributed in the area east of Ban Huai Kaeo in the northeastern part of the surveyed area. They are biotite granite showing porphyritic texture with big phenocrysts of feldspar. Under microscope, there are many coarse grained hypidiomorphic crystals, and the rock is composed of idiomorphic quartz more than 4 mm in diameter, hypidiomorphic plagioclase showing albite twins, hypidiomorphic perthite and pleochroic biotite. As accessory minerals, zircon, apatite, sphene and magnetite are recognized.

By the result of the age determination of this rock by K-Ar method, the value of age is 212 ± 10 m.y. and the period of the intrusion is taken to be at the end of Triassic (Table II.1.1-2).

4-2-4 Alluvium

Along the Nam Mae On River in the central to southern part of the surveyed area, and along the streams near Ban Pong Hom in the northwestern part of the surveyed area, alluvium deposits are well developed and the land is utilized for rice field. The alluvium is composed of clastic deposits supplied from various rocks distributed in the surrounding area. The thickness is estimated to be less than 10 meters in most part.

4-3 Geological structure

4-3-1 Structural characteristics

The surveyed area is situated, viewing from the tectonic provinces, in the western marginal zone of the Central North Tectonic Province (Fig. II.1.1-2). The province is composed of the volcanic rocks of calc-alkali series effused in the period of middle Paleozoic to early Mesozoic, and of the sedimentary rocks of the facies of continental margin. The province is characterized by the intense folding structure and thrust faults. The beds in this province have been dislocated by faulting and folding. The Chiang Mai basin is one of the Cenozoic sedimentary basin in the inland area in the northern part of the Kingdom of Thailand, and viewing from the characteristic fissure systems in half circular arc and concentration of epicenters of the earthquakes, it is thought that the structural movement is active in this area.

The San Kampaeng geothermal area is located next to the Chiang Mai basin in its east, and it is thought that there would be some influence on the structure in the area by the active structural

movement in the neighbouring basin.

The surveyed area is topographically composed of the western mountaneous land, the central lowland and the eastern mountaneous land. The western mountaneous land lies at the altitude of 500 to 650 meters above sea level, from Doi Luang to Doi Sam Ngok. The central lowland lies at the altitude of 350 to 450 meters above sea level and occupies the basin areas of the Nam Mae On River flowing southward and of the Huai Ang River which runs toward north. The lowland has width of several kilometers, with small hill or small range of hilly land found in the western part. The eastern mountaneous land includes the range at the altitude of more than 500 meters. It is broader and higher land than the western mountaneous land. These topographical arrangement is thought to be in good harmony with the characteristics of the geological structure stated hereafter.

The subject area is divided into three structural units by the main faults; Doi Luang uplifted zone, Ban Pong Hom subsided zone and Mae Tha uplifted zone. The faults bordering the three units are the Huai Pong fault and the Huai Mae Koen fault, both of which are normal faults, trending in NNW-SSE direction.

The Doi Luang uplifted zone is corresponding roughly to the western mountaneous land. This uplifted zone is composed of massive sandstones of the Carboniferous Mae Tha Formation. Faults of the trends of NW-SE, E-W and N-S are well developed in this zone. Foldings with the axes in the direction of NW-SE are also recognized.

The Ban Pong Hom subsided zone is corresponding to the central lowland. In the western part of this subsided zone, the sedimentary rocks (sandstone, shale, limestone and chert etc.) of middle to lower part of the Kiu Lom Formation of the Permian period are distributed, while the eastern part is occupied by the basaltic lava and pyroclastic rocks of the upper part of the Kiu Lom Formation. The faults of the trends of NNE-SSW, NNW-SSE and NW-SE are well developed in this zone. Although folding structures are recognized in some parts with the axes in the same directions as the trends of the major faults, geological structure in this zone is taken as monocline, as a whole, dipping to the east. The dips of the beds are as steep as 50 to 80°, generally.

The Mae Tha uplifted zone is corresponding to the eastern mountaneous land. This uplifted zone is composed of sandstones of the Mae Tha Formation, shales of the lower part of the Kiu Lom Formation, and granites intruding the Mae Tha Formation. Faults of NNW-SSE trend are prevailing, but there are some faults trending in NE-SW or E-W direction, which have been cut by the former faults. Also, foldings with the axes in N-S or NW-SE direction are developed. Thus, the Doi Luang uplifted zone and the Mae Tha uplifted zone have quite a good similarlity each other, viewing from the lithofacies of the component rocks and the characteristics of the geological structure.

4-3-2 Fissure system

In this surveyed area, there are many faults of various trends such as NNW-SSE, NNE-SSW, NW-SE, NE-SW and E-W. Of them, the faults of the trend of NNW-SSE are significant for the geological structure. Above-mentioned Huai Pong fault and Huai Mae Koen fault are two of such significant faults. The three faults of the trend of NW-SE, recognized from Ban Pong Nok to the upstream area of the Huai Ang River, are thought to be the branched faults formed with the Huai Pong fault. The fault planes of the faults in this area including the Huai Pong fault and the Huai

Mae Koen fault are rarely observable. However, as the extension of the faults on the surface is straight in many cases, it is inferred that they have quite steep dipping angles and that they are normal faults probably.

The subject area is divided into three structural units by the Huai Pong fault and the Huai Mae Koen fault: the Doi Luang uplifted zone, the Ban Pong Hom subsided zone and Mae Tha uplifted zone. The faults developed in each structural zone, having trends of NW-SE, NE-SW and E-W, are distributed exclusively in each structural zone, and they do not extend beyond the Huai Pong fault or the Huai Mae Koen fault.

There are some other tectonic elements than those stated in the above paragraphs, in the surveyed area. One of these structural elements is pointed out to be joints, which have been filled with quartz veins. The trends of the quartz veins are predominantly in E-W direction, although there are some which are trending in NNW-SSE direction. Most of the E-W trending joints are to cross the folding axes, and they are thought to be tensional cracks formed with folding movement.

It is recognized that the characters of the fissures and cracks are different according to the properties of the beds. That is, the quartzose sandstone of the Mae Tha Formation and the basaltic lava and pyroclastic rocks of the upper part of the Kiu Lom Formation are comparatively homogeneous and massive, rarely containing fissures. On the other hand, the sedimentary rocks of the middle to lower part of the Kiu Lom Formation are vertically heterogeneous because they have alternation structure. They contain comparatively fine fissilities, though large-scaled joints are rarely developed. Especially, the chert has high fragility and is often brecciated into small pieces. Also the sitstone is easily weathered and altered, to form white and soft rock, containing many fissilities.

4-3-3 Folding structure

Generally, folding structures are well developed in this surveyed area. Intensity and pattern of the foldings are different in each structural zone.

In the Doi Luang uplifted zone and in the Mae Tha uplifted zone, foldings have been formed closely one another, repeating synclines and anticlines with the wave length of 400 meters to 1 kilometer. The folding axes are almost flat, showing trends of NW-SE or NNW-SSE. The dips of the beds are as gentle as 40 to 60°.

In the Ban Pong Hom subsided zone, folding structures are not remarkable, and the homoclinal structure is characteristic, dipping 50–80° to the east. The folding structures, recognized in the western part and in the central part of this zone, have flat to gently dipping folding axes, with the trend of NNE-SSW.

4-4 Alteration zones

4-4-1 Results of X-ray analysis and the distribution of alteration zones

The alteration survey was carried out in an area of approximate 2 km^2 around the area where the geothermal indications are distributed. X-ray analysis was completed with the 103 samples collected in this survey (Table II.1.1-3).

The detected clay minerals are halloysite, montmorillonite, saponite, sericite, chlorite, kaolinite, and alunite. Gypsum, jarosite and pyrite are also recognized.

Table II.1.1-3 X-ray diffraction data of altered rocks (1)

No.	Constituent Mineral / Sample Number	Quartz	Calcite	Plagioclase	K-feldspar			Halloysite	Montmorillonite	Saponite	Sericite	Chlorite	Kaolinite	Alunite	Gypsum	Jarosite	Marcasite	Pyrite	Goethite	Gibbsite		Rutile	Anatase	Hornblende?	Stilpnomelane?
1	T-056	◎		◎	•				◎			>			•			>						>	
2	T-057	◎	>	◎	•				>			>			>			>						>	
3	T-058	◎		◎	•				◎			>			>			>						>	
4	T-059	◎		◎	•				◎			>			>			>						>	
5	T-060	◎		◎	•				◎			>			>			>						>	
6	T-061	◎		○	•				◎			>			>			○						>	
7	T-062	○		◎	•				◎			•			>	•		>						•	
8	T-063	>		◎	•				◎			>			>			○						>	
9	T-064	◎	◎	◎	•				◎			>			•			>						>	
10	T-065	◎		◎	•				◎			>			•			>						•	
11	T-066	○		◎	•				◎			○			•			○						>	
12	T-067	◎		◎	•				◎			>			•			>						>	
13	T-068	△		◎	•				△			△			>	•		◎						>	
14	T-069	◎		>					◎						>	>		>						•	
15	T-070	△	○	○	△				◎			○						○						>	
16	T-071	◎		◎					>		•	>			•			>						>	
17	T-072	◎		◎	•				>	•		>			•			>						>	
18	T-073	◎		◎	•				○	•		>			>			>						>	
19	T-074	◎		>	•				○	○		>			•			>						>	
20	T-075	•	◎	>					○	○		>			•			>						•	
21	T-076	◎		○	•				◎	◎		>			>			>						>	
22	T-077	◎									>		•												
23	T-078	◎		>					○		•		•		>	•		>						•	
24	T-079	◎		>					◎									○							
25	T-081	◎									>		>						•						
26	T-087	◎									○		>						•						
27	T-091	◎									○	>	○						•			•			
28	T-097	◎	•	◎	○							◎								○					○
29	T-104	◎									>		◎										•		
30	E-002	◎									>		>												
31	E-003	◎									>		>						>						
32	E-010	◎									○		○										>		
33	E-011	◎			◎						>		>												
34	E-014	◎									○		○										•		
35	W-004	◎									○		>												
36	W-021	△		○					○				>						>						
37	W-022	○		○					◎				>												
38	W-024	◎									○		◎						>						
39	W-025	◎									○		○						•				•		
40	W-026	◎									◎		○						>						

Table II.1.1-3 X-ray diffraction data of altered rocks (2)

No.	Constituent Mineral / Sample Number	Quartz	Calcite	Plagioclase	K-feldspar		Halloysite	Montmorillonite	Saponite	Sericite	Chlorite	Kaolinite	Alunite	Gypsum	Jarosite	Marcasite	Pyrite	Goethite	Gibbsite		Rutile	Anatase	Hornblende?	Stilpnomelane?
41	W-027	◎								○		○										・		
42	W-028	◎										∧						○				∧		
43	W-029	◎								∧		∧						○						
44	W-030	◎								△		∧						∧				△		
45	W-031	◎					○			・								∧				∧		
46	W-032	◎					○											○				○		
47	W-033	◎					∧			・								○						
48	W-034	◎					△			△								○				∧		
49	W-035	◎					∧			∧								∧				・		
50	W-036	◎					○			○								・				△		
51	T-003								◎														・	
52	T-004	・		◎					∧		・		・				・							∧
53	T-007	◎											◎								・			
54	T-009	◎		○				∧		・		・					・						・	
55	T-010	◎		△	・					・		・		∧									・	
56	T-011	◎		△				○		・		・		・			∧							
57	T-012	◎		△				○		・		・		・			∧							
58	T-013	◎		△				○		・	・			・			△						・	
59	T-014	◎		△				◎		・				・			∧							
60	T-015	◎		○				∧		・	・			・			○						・	
61	T-016	◎		○				∧		・	・			・			∧						・	
62	T-017	◎		∧				∧		・				・			∧						・	
63	T-018	◎		○				∧		・	・			・			○						・	
64	T-019	◎		△				△		・	・	・		∧			△						・	
65	T-020	◎	○	△				△		・	・			∧			∧						・	
66	T-021	◎						△		・				∧			・							
67	T-022	◎		△						・							∧							
68	T-023	◎						△		・	・			・			△						・	
69	T-024	◎		△				△						・			・							
70	T-025	◎		△				△						・			△							
71	T-026	◎		△				∧				・		・			∧							
72	T-027	◎		△				∧		・	・			∧			∧							
73	T-028	◎		△				△		・		・		∧			∧						・	
74	T-029	◎		△				○		・		・		・			・						・	
75	T-030	◎		△				○		・		・		∧			∧						・	
76	T-031	◎		△				△		・		・		∧			△						・	
77	T-032	◎		△				∧		・		・		∧			△						・	
78	T-033	◎		△				∧		・	・			∧			∧						・	
79	T-034	◎		○				◎			△			・			∧						・	
80	T-035	○		◎	・			◎			・						∧						・	

Table II.1.1-3 X-ray diffraction data of altered rocks (3)

№	Constituent Mineral / Sample Number	Quartz	Calcite	Plagioclase	K-feldspar	Pyroxene(Augite)	Biotite	Montmorillonite	Saponite	Sericite	Chlorite	Kaolinite	Alunite	Gypsum	Jarosite	Marcasite	Pyrite	Sphene	Gibbsite	Pumpellyite ?	Rutile	Anatase	Hornblende?	Stilpnomelane?
81	T-036	◎		◎	•			◎			•			△			△						•	
82	T-037	◎		◎	•			○			•		•	△			△						•	
83	T-038	◎		◎	•			○						•		○	○						•	
84	T-039	◎		◎	•			○			•			△	△		△						△	
85	T-040	◎	◎	○	•			△			△			•			△						•	
86	T-041	○		◎	•			△			△			△			△						△	
87	T-042	◎		◎	•			◎			△			△	•		△						△	
88	T-043	◎		◎	•			◎			△			•			△						△	
89	T-044	◎		◎	•			△			•			•	△		○		△				△	
90	T-045	◎		◎	•			○			△			•			△						△	
91	T-046	◎	△	◎	•			△			△			△			△						△	
92	T-047	◎		◎	•			○			△			△			△						△	
93	T-048	◎	○	◎	•			○			△			△			△						△	
94	T-049	◎		◎	•			◎			△			•			△						△	
95	T-050	◎		◎	•			◎			•			△			△						△	
96	T-051	◎		○				◎							△									
97	T-052	◎		◎	•			△			△			△	•		○						△	
98	T-053	◎		◎	•			○			△			△			△						△	
99	T-054	△		◎	•			△			△			△			△						△	
100	T-055	◎		◎	•			◎			△						△							
101	T-001	•				◎					◎						•	△		△			•	
102	T-080	△		◎		○					△													
103	W-019	•		◎		○	•				△		•											

◎ Abundant
◎ Much
○ Common
△ Few
• Very rare

As the rock forming minerals, quartz, calcite, plagioclase, kali-feldspar, hornblende, anatase and stilpnomelane are recognized.

From the results of the microscopic observation, quartz, chlorite and sericite are contained in fair amount in the rocks. Accordingly, while these minerals are detected by the X-ray analysis, it is difficult to determine whether they are originated from the alteration or from the original rocks.

Therefore, for the examination of the zonal distribution of the alteration, sericite and chlorite were excluded. Based upon the assemblage of the clay minerals without the above two, alteration zones have been divided as follows (PL II.1.1-6).

(1) Alunite zone
component mineral: alunite, saponite

(2) Kaolinite zone
component mineral: kaolinite (sericite)

(3) Kaolinite-montmorillonite zone
component mineral: kaolinite, montmorillonite
(sericite and chlorite are contained in some cases)

(4) Montmorillonite zone
component mineral: montmorillonite, saponite
(sericite and chlorite are contained in some cases)

(5) Halloysite zone
component mineral: halloysite
(sericite is contained in some cases)

Alunite has been recognized only at a point about 30 meters south of the site where the geothermal exploration well GTE-2 is located, associated with saponite. Accordingly, extension or distribution of the alunite zone is not obvious, although possibly it extends in south.

The kaolinite zone is distributed in east and west, around the site of GTE-2 and in its east-side area. The zone is also recognized in the north of Ban Pong Hom and along the road at the foot of the mountains in the western part.

The kaolinite-montmorillonite zone is recognized at around the hot spring about 80 meters northwest of the point of GTE-2, and also about 400 meters east of the point. The zone extends in east and west, neighbouring to the north of the kaolinite zone.

The montmorillonite zone is recognized in and around the area where principal hot springs are distributed, along the Huai Mae Khu Ha River. It has approximate width of 200 meters and extends in east and west.

The halloysite zone is recognized around Wat Pong Hom and at around the point about 400 meters southeast of Ban Pong Hom. The extension of the distribution of this zone is in E-W or NW-SE direction.

4-4-2 Elucidation of the Alteration zones

Generally, it is thought that assemblages of alteration minerals in geothermal area are controled by chemical composition and temperature of hydrothermal liquid.

Also, stable area of alteration minerals for temperature depends upon temperature as shown in Fig. II.1.1-3, although it differs by pH of the hydrothermal liquid.

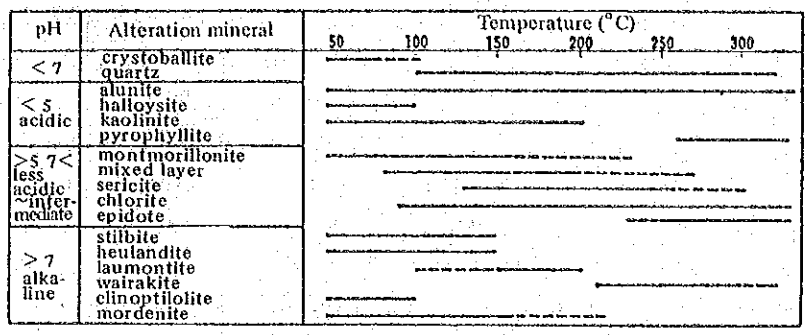

Fig. II.1.1-3 Stable area of alteration minerals for temperature

Judging from the dependance of temperature of the alteration minerals, the hydrothermal solution causing alteration in this area is thought possibly to be intermediate to acidic liquid of the temperature of less than 200°C.

As for the alteration, zonal distribution of the alteration is observed in the following order.

alunite zone

kaolinite zone

kaolinite – montmorillonite zone

montmorillonite zone

halloysite zone

It is thought as for this zonal distribution that, from the alunite zone toward the halloysite zone, the temperature of the hydrothermal solution would have been decreasing and that the solution would have changed its acidic property to the intermediate one gradually.

The alteration zones are distributed extending in the direction of east and west, and their distribution reveals the change of the character of the solution from the high temperature type to the low temperature type, toward the north from the south of the point of GTE-2. Also the area, where present hot springs are distributed, is included in the range from the alunite zone to the montmorillonite zone. This is taken to show that the distribution of the alteration zones have intimate relation to the present activity of the hot springs. The alunite zone confirmed in this alteration survey is noted to indicate that the center of the alteration would be at the south of the point of GTE-2.

The kaolinite zone, found near Ban Pong Hom, seems to be independent from the area where the geothermal indications are distributed. It is thought that this kaolinite zone would possibly have been formed through some separated passages from those with the actual geothermal activities or by some other geothermal activities in different period.

5. Summary

Along the main routes in the surveyed area, geological mapping and alteration surveys were carried out, using the topographical map of the scale of 1 to 10,000. The rock samples collected in these surveys were supplied to the laboratory examination such as microscopic observation, fossil determination, age determination and X-ray diffraction analysis, according to the subject of the samples. By the results of the fieldworks and the laboratory examinations, the geological maps, the geological profiles and the zonal distribution map of alteration zones were drawn up. The contents shown in the following paragraphs have been clarified as the results of the geological survey.

The surveyed area is underlain, from the lowest, by the Carboniferous Mae Tha Formation, middle Permian Kiu Lom Formation, Triassic granites and alluvial deposits. The Mae Tha Formation is distributed in the western and eastern mountaneous land, and is composed mainly of white, massive and medium grained sandstones, although it contains thin layers of black shale as insertions in the eastern part. The thickness is more than 1,600 meters. The Kiu Lom Formation is distributed in the central lowland and in the eastern mountaneous land. It is inferred that this formation is in contact with the underlying Mae Tha Formation with unconformity, although they are bounded by faults in the field. This formation is divided, from the lithofacies, into three parts; the lower part, the middle part and the upper part. The lower part is divided into the alternation of limestone and shale, the sandstone bed, the alternation of siltstone, sandstone and chert, the chert bed, and the alternation of siltstone and sandstone. The thickness of the lower part is over 1,360 meters. The middle part is composed of basaltic lava, tuff in the lower half and limestone, shale in the upper half. The thickness is about 800 meters. The upper part is represented by the basaltic lava, lapilli tuff and tuff breccia, though layers of tuffaceous sandstone, chert and siltstone are inserted partly. The thickness of this part is as thick as 6,500 meters. The granites are distributed in the northeastern part of the surveyed area. They are porphyritic biotite with large phenocrysts of feldspar. Alluvium deposits are developed along the main rivers in the surveyed area. The thickness of the alluvium is as thin as less than 10 meters.

The surveyed area is divided into three structural units by the Huai Pong fault and the Huai Mae Koen fault, both of which are trending in NNW-SSE direction. The three structural units are Doi Luang uplifted zone (western mountaneous land), Ban Pong Hom subsided zone (central lowland) and Mae Tha uplifted zone (eastern mountaneous land). The Doi Luang uplifted zone is composed of massive sandstones of the Carboniferous Mae Tha Formation. Faults of the trends of NW-SE, E-W and N-S and foldings with the axes in the direction of NW-SE are well developed. The Ban Pong Hom subsided zone is composed of marine sediments and basalts belonging to the Permian Kiu Lom Formation. Faults of the trends of NNE-SSW, NNW-SSE and NW-SE are well developed. Although folding structure is recognized in some part, geological structure in this zone is homoclinic as a whole, dipping to the east. The Mae Tha uplifted zone is composed of sandstones of the Mae Tha Formation and shales of the lower part of the Kiu Lom Formation. Intrusion of Triassic granites is recognized in the northeastern part of the area. Faults of the trend of NNW-SSE are prevailing and foldings with the axes of N-S or NW-SE are developed.

Alteration zones are distributed in and around the area where the present geothermal indications are distributed, and are revealing anomalous structure extending in east and west or in northwest and southeast. Zonal arrangement is obviously recognized as follows, based upon the assemblage of the clay minerals: alunite zone (south side), kaolinite zone, kaolinite-montmorillonite zone, montmorillonite zone, and halloysite zone (north side). It is inferred that the hydrothermal solution, which has brought about such zonal distribution of alteration, would have changed its own character from acidic to intermediate, and its own temperature from higher to lower, toward the north from the southern side.

Geologically, the most important factor ruling the geothermal reservoir is thought to be fissures in the beds. In another word, it is thought that the forms of the geothermal reservoir and amount of the hydrothermal solution are depending upon the distribution of open cracks in the rocks.

By the present geological survey, it has been clarified that the important factors are well-fractured beds and fractuated zones associated with faults, being favorable for geothermal reservoir. As for the faults, it is the Huai Pong fault and the faults of NW-SE trend, branched from the former, in the southern area of the area where the geothermal indications are distributed, that are thought to be related to geothermal reservoir. The well-fractured beds are those easily fractured at the period of structural movement. In this surveyed area, they are chert and siltstones of the Kiu Lom Formation. It is thought that the upflow of the geothermal fluid occurs mainly along fractured zones associated with faults, and that the faults and in some part, cracks in chert and siltstone would play important roles for the reservation of geothermal fluid.

The existence of the alteration zones is thought to indicate past activities of geothermal fluid. The distribution of the alteration zones and that of the geothermal indications are almost corresponding each other, when a glance is given to whole of the surveyed area. However, viewing them in detail, the distribution of alteration zones is broader and its center is located a little south of the area of the distribution of the geothermal indications. These facts are thought to suggest that the center of the hydrothermal activities has moved northward in the course of time.

II-1-2 Gravity Survey

1. Foreword

Gravity survey is a method to estimate underground structure by measuring gravity anomaly, caused by the heterogeneous distribution of density below surface.

That is, the gravity survey is a method to get information of rock distribution, depth and top of the basement, location and size of the intrusive bodies and the existence of structural lines such as faults and fractured zones. This survey is effective to have general comprehension of the geological structure in whole of an area.

For the geothermal exploration, it is expected by the survey to estimate underground structure represented by fault and subsidence, which controls existence of geothermal fluid, and to detect geothermal reservoir and intrusive bodies, which are directly related to the geothermal resources.

It is thought in the geothermal area that there are different patterns of gravity anomalies according to the types of geothermal reservoir. In the geothermal area such as Larderello and Monte Amiata in Italy, the main vapor-production zones are situated on the steep slope of gravity anomalies.

The process of works in this gravity survey, from the gravity measurement to the report, is shown in Fig. II.1.2-1.

2. Field survey

2-1 Gravimeter

The gravimeters used for the present gravity survey are G-283 and G-366, made by La Coste & Romberg.

These gravimeters have graduation of 0 to 7,000 and the gravity values of 0 m gal to appromate 7,400 mgals can be measured. The precision of measurement is as high as ± 0.01 mgals.

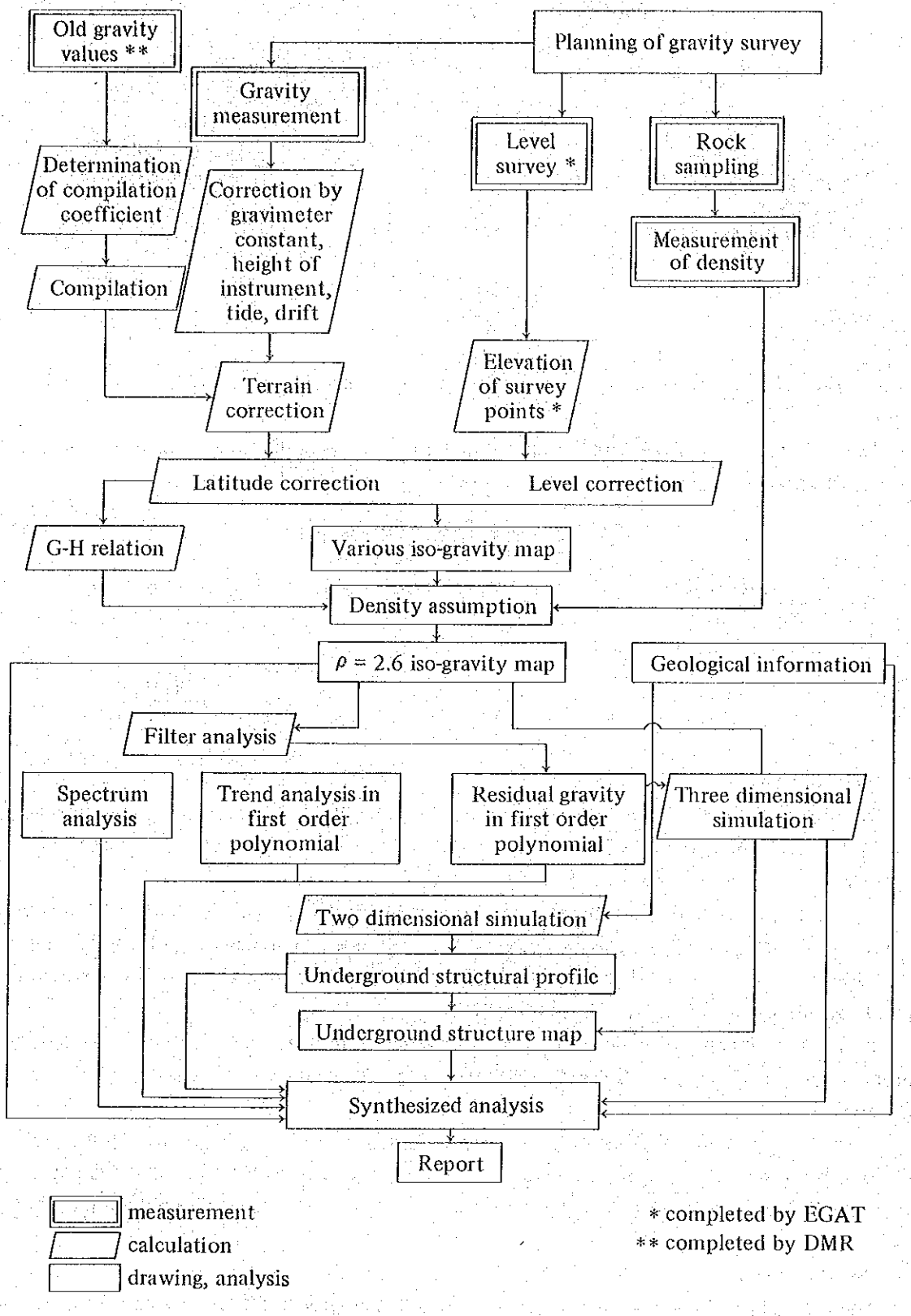

Fig. II.1.2-1 Flow chart of the gravity survey

Table II.1.2-1 Specification of gravimeter

Name, type	La Coste & Romberg, INC. Model G Geodetic Gravity Meter	
No.	283	366
Measurement range	0 ~ 7,386.54 m-gal	0 ~ 7,404.56 m-gal
Temperature of thermostat cell	51.7°C	49.0°C
Reading line	2.80	2.90
Date of purchase	September 1971 (overwhole June, 1981)	September 1974
Size	14 x 15 x 20 (cm)	17 x 15 x 22 (cm)
Weight	8.6 kg	9.1 kg

Also as the drift ratio is extremely small as less than 1 mgal/month, a base tie per day is sufficient.

The following table of gravimeter constants is a part of the table to exchange counter reading values with gravity values.

Table II.1.2-2 Gravimeter constants

Counter reading	Value in milligal	Factor for interval
2,700	2,847.21	1.05550
2,800	2,952.76	1.05559
2,900	3,058.32	1.05568
3,000	3,269.46	1.05587

2-2 Base station

To correct the drift of the gravimeters, base tie is required. For this purpose, a base station for the base tie, No. 1000, was set on the concrete floor at the entrance of the lodge of the clinic, about 100 meters west of the EGAT camp.

The datum value of the gravity can not be obtained around the surveyed area, and the control point established when DMR carried out gravity survey in the area including Chiang Mai has been lost already. Therefore, the survey results (gravity values) obtained in this survey is not able to be tied to another survey (gravity values) directly.

As the datum value of gravity requires latitude correction, the standard gravity value at the base station No. 1000, S.V. 1000 = 978,497.981 mgals, was taken to be tentative datum value of the gravity.

When datum value of gravity should be established in future, it is possible to integrate the gravity values and the bouguer anomalies to any other data by correcting all the gravity values with the difference between the above tentative datum value and the established datum value.

2-3 Survey points

The area where the gravity survey was carried out is as large as 50 km^2 around the area where the geothermal indications are distributed. To get clear informations on the geological structure in whole of the area and to draw up such structures as to control the existence of geothermal resources, it is desirable to survey the area as broad as possible, while the distribution of survey points should be as dense as possible. Gravity survey had been conducted by Thailand side in the

plains in this surveyed area, but as the area surveyed was so small and the survey points were uncertain when planning the present survey program, the independent program of the point distribution was employed and the survey was carried out according to this program.

The survey lines, which had been prepared by bush-cutting by Thailand side in the central part of the surveyed area were employed as much as possible. In other parts, roads were utilized as survey lines, from the viewpoint of the efficiency of the level survey. As a whole, the survey points were established with intervals of 400 ~ 600 meters.

The determination of the survey points was based on the topographical map of the scale of 1 to 10,000, but as the location of the roads was different from that indicated on the map, land survey was conducted by the measuring tape and simplified transit compass, to locate the survey points along the roads after drawing up the figures of these roads, rendering the cut-lines to the base.

2-4 Level survey

Level survey was carried out for all of the survey points by EGAT level survey crew. The elevation of the base point BMCS-18, which is 392.418 m, located in the EGAT camp, was employed as the elevation of the control point.

As the level survey had been completed partially along the cut lines, the survey started at the end point of the former survey. Staff was moved twice and the reading was also done twice, as most of the lines were programmed to be open.

2-5 Collection of rock samples

For the analysis and the terrain correction of the gravity values, rock samples distributed in the surveyed area were collected and the average density was measured with them.

Total 84 rock samples were collected, of which 65 samples were from the surface outcrops and the other 19 samples were from the drill core. These rock samples were brought back to Japan for the measurement of the density.

3. Method of analysis

3-1 Correction of gravity values

Gravity values measured are within influences of various heterogeneous factors such as time, location, elevation, relative features of topography and so on.

To obtain real gravity values under uniform condition, these factors should be corrected. In this survey, correction was performed with such factors as tide, height of instrument, drift, lattitude, terrain, free air and bouguer, etc. Calculation for these corrections was completed by the electronic computer of FACOM M160-AD type. Principal methods of correction and data processing are stated in the following.

3-1-1 Tidal correction

Tidal correction is to eliminate influence of the variation of the positions of the moon and the sun to the gravity measurement. The correction is different according to time and latitude of the survey points. By this tidal correction of all the measured values, it is possible to regard the drift correction to be simple base tie error. Thus, precision can be improved.

The relations between time and positions of the moon and the sun are read from "Abridged Nautical Armanac" published by The Maritime Safety Agency of Japan. The following formula was employed for the calculation.

$$\Delta g = \frac{3}{2} GM \frac{a}{\gamma^3} \left\{ 3\left(\sin^2\delta - \frac{1}{3}\right)\left(\sin^2\varphi - \frac{1}{3}\right) + \sin 2\delta \ \sin 2\varphi \ \cos\theta + \cos^2\delta \ \cos^2\varphi \ \cos 2\theta \right\}$$

Here the symbols stand for

G : universal gravitation constant (6.67×10^{-11} $m^3/kg\ sec^2$)

M : mass of celestial object the moon : 7.348×10^{22} kg
the sun : 1.9891×10^{30} kg

a : distance from the center of the earth to the survey point
$= 6{,}378.388(0.99832 + 1.6835 \times 10^{3} \ \cos 2\varphi - 3.5 \times 10 \ \cos 4\varphi)$
+ (elevation of the survey point in km)

γ : distance from the center of the earth to the celestial object
(the moon ; 384,405 km, the sun ; 1.496×10^{8} km)

φ : latitude of the survey point

δ : declination of celestial object (angle measured in northsouth to the equator)

θ : hour angle of celestial object
(angle between the celestian meridian and the survey point meridian)

3-1-2 Drift correction

After measuring gravity values of new survey points starting from the point with known value of gravity, the original gravity value can not be obtained usually when returened to the starting point, even if tidal correction and height-of-instrument correction are completed. The difference is called to be "drift".

Though La Coste gravimeter has very little error caused by temperature and atmospheric pressure, it has drift concerning spring fixing system with the lapse of time.

Drift correction was done in each base tie, taking the drift to be in proportion to lapse of time. The highest value of drift was 0.074 mgals/day on 7th of December, 1982.

3-1-3 Terrain correction

Terrain correction is required in order to eliminate influence of topography around the survey point to the gravimeter. Land is divided by grid with certain space on the topographical map. The elevation of the central point of each grid is read, and relative undulation of these values of elevation to that of the survey points can be approximated to a certain shape. The sum of the gravity values affected by these correction grids is taken to be terrain correction value.

The more influence of topography is seen, the nearer the terrain is to the survey point, and the influence is smaller with the increase of distance from the subject terrain to the survey point. Therefore, correction of high precision was done with such terrains close to the survey point, while correction was comparatively rough with terrains far from the survey point.

Area of the correction is designed taking it into consideration that the surveyed area is flat and surrounded by hilly land. The outline of the calculation domain of the terrain correction, area of correction and the spacing of the grid around a survey point are given as follows.

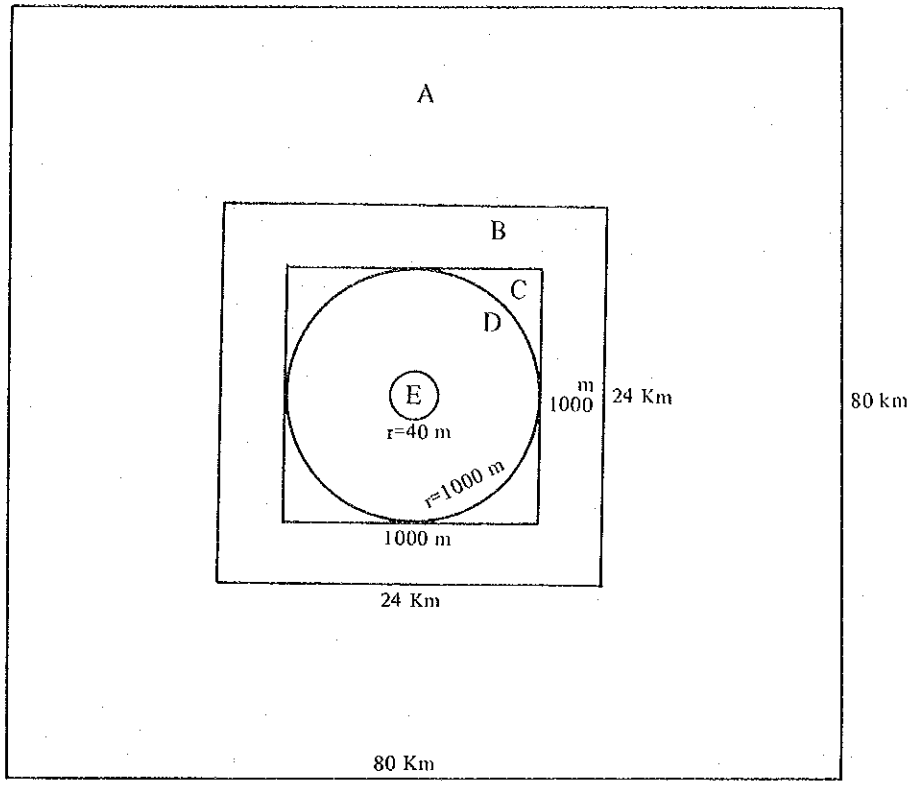

Fig. II.1.2-2 Domains of calculation of the terrain correction

As the data for terrain correction of "far" and "middle", topographical mesh data were prepared by reading elevation of the crossing point of grid on the topographical map, after establishing grid with the employed spacing (Table II.1.2-3) on the topographical map, in the designed area for the correction of all the survey points. The relation of the used topographical map of the scale of 1 to 50,000 and the designed area for the correction of all the survey point is shown in Fig. II.1.2-3.

Table II.1.2-3 Outline of the terrain correction

Name	Do-main	Method of correction	Area of correc-tion with a survey point	Grid spacing of topographical mesh data	Topographical map
far	A	cocentric circle cylinder approximation	80 km (E-W) x 80 km (N-S)	2000 m (E-W) x 2000 m (N-S)	1/50,000
middle	B	as above	24 km (E-W) x 24 km (N-S)	500 m (E-W) x 500 m (E-W)	1/50,000
near (1)	C	pentahedron approximation	in neighbor (2) and its circumscribed quadrilateral	refer to map	1/50,000
near	D	cocentric circle cylinder reading	within 1000 m of radius around the survey point	as above	1/10,000
close	E	profile approximation	within 40 m of radius around the survey point	—	sketch 1/500

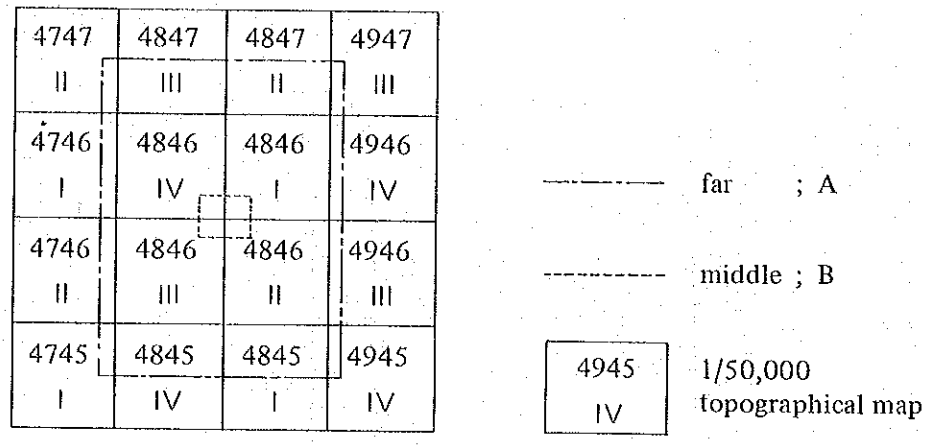

Fig. II.1.2-3 Topographical map and area of terrain correction

As the topographical mesh data prepared are without relation to the locations of the survey points, they are different from the grid for calculation of the terrain correction, which is based upon the location of respective survey points. The elevation of the center of the grid for calculation necessary to the terrain correction is obtained according to the following formula, using weight of the distance from the topographical mesh data to the center of the grid.

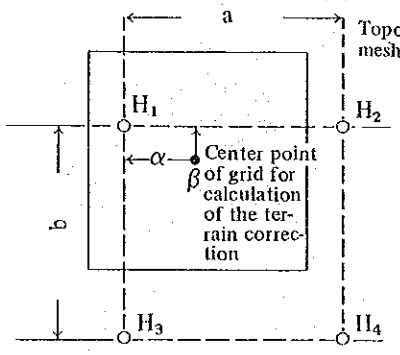

$$\bar{H} = H_1 + (H_2 - H_1)\frac{\alpha}{a} + (H_3 - H_1)\frac{\beta}{b} + (H_1 + H_4 - H_2 - H_3)\frac{\alpha \cdot \beta}{a \cdot b}$$

Fig. II.1.2-4 Elevation of grid points

Calculation of the terrain correction was performed by the following formula, after replacing the section, for which calculation of the terrain correction is applied, by a concentric circle cylinder having the same area (Fig. II.1.2-5).

The correction of the "near (1)" was done by pentahedron approximation (Fig. II.1.2-6) with the pentahedral intermediate area, composed of the circle with the radius of 1000 meters from the survey point and its circumscribed quadrilateral, using the elavation of the lattice points of the topographical mesh and the survey points.

The correction of the "near (2)" was done depending upon Hammer's approximation formula (Fig. II.1.2-8), after reading, on topographical map of the scale of 1 to 10,000 (Fig.II.1.2-7), the average elevation of the section prepared by dividing the area between the circles of the radius of 40 m and 1,000 m into concentric circle cylinders.

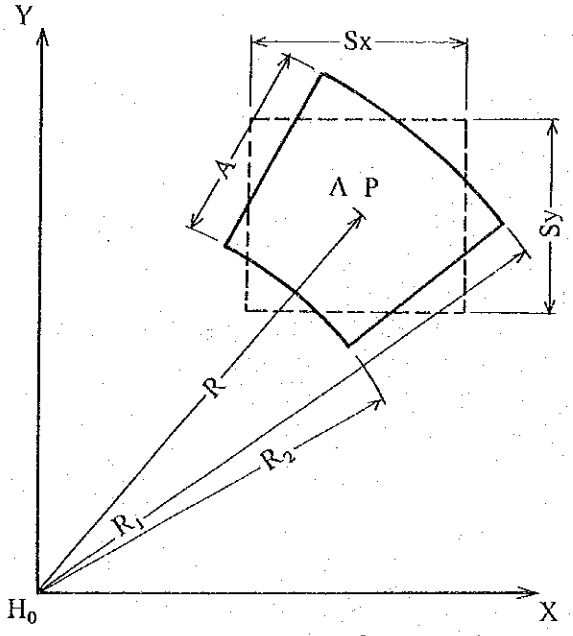

$$\Delta g = \frac{2G\rho A^2 (R_2 - R_1 + \sqrt{R_1^2 + H_1^2} - \sqrt{R_2^2 + H^2}}{R_2^2 - R_1^2}$$

Δg: value of terrain correction
G: gravity constant (6.670×10^{-8} dyne cm^2/g^2).
ρ: density
A^2: area of the section of correction
H: difference between the average elevation of the section of correction and the elevation of the survey point, $\overline{H} - H$.
A: $\sqrt{Sx \cdot Sy}$
R_1: $R - A/2$
R_2: $R + A/2$

Fig. II.1.2-5 Calculation of the terrain correction

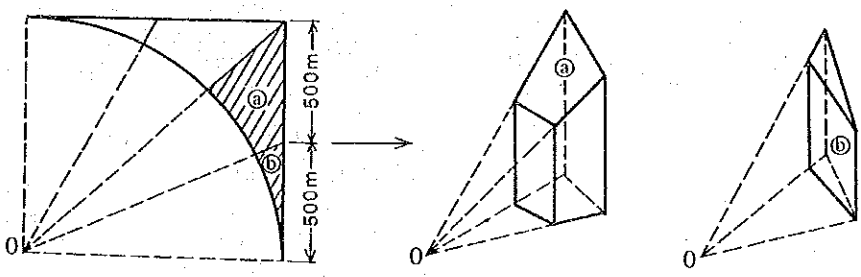

Fig. II.1.2-6 Pentahedron approximation

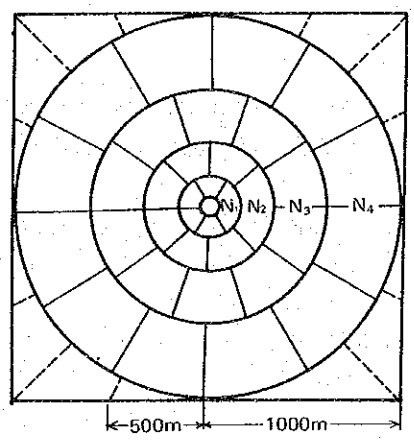

Area of correction (distance from the center: m)		Number of section of cocentric circle
	$(R_1) \sim (R_2)$	(n)
N_1	40 ~ 150	6
N_2	150 ~ 340	8
N_3	340 ~ 620	10
N_4	620 ~ 1000	12
(Total)		(36)

Fig. II.1.2-7. Terrain correction of the near (2)

$$g = \frac{2\pi G\rho}{n}(R_2 - R_1 + \sqrt{R_1^2 + H^2} - \sqrt{R_2^2 + H^2})$$

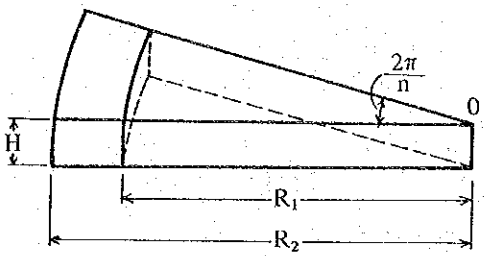

g: value of terrain correction
G: gravity constant
ρ: density
R_1: inside diameter
R_2: outside diameter
H: difference of elevation between the survey point and the section for correction
n: number of equal parts divided

Fig. II.1.2-8 Hammer's approximation formula

The correction of the "close" was done by the calculation according to the following formula (Fig. II.1.2-9), after preparation of profile sketches, along two lines across the survey point, of the topographical features in the area within 40 m of radius from the point.

$$\Delta g = 2G\rho \int \left\{ \tanh^{-1} \sqrt{\frac{R^2 - X^2}{R^2 + H_0^2}} - \tanh^{-1} \sqrt{\frac{R^2 - X^2}{R^2 + (X\tan\beta + H - H_0 - D\tan\beta)^2}} \right\} dX$$

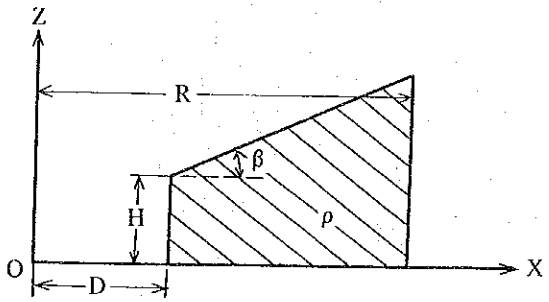

Δg: value of terrain correction
G: gravity constant
ρ: density
D: distance from survey point to cliff
H: height of cliff
β : angle of inclination
R: area of correction
H_0: height of plumb of gravimeter (0.15 m)

Fig. II.1.2-9 Correction of close

3-1-4 Elevation correction

The elevation correction includes free-air correction, which is to correct gravity values with the difference of elevation, and bouguer correction, which is to correct influence of density of rocks in the underground.

Free-air correction value Δg_1 is obtained by the following formula, using average vertical gravity gradient on the surface of the earth.

$$\Delta g_1 = g_0 \left\{ 1 - \frac{R^2}{(R+H)^2} = \frac{2g_0 HR + g_0 H^2}{(R+H)^2} \right\} \simeq \frac{2g_0}{R} H \doteqdot 0.3086H \text{ mgals}$$

Here symbols stand for

g_0 : mean sea level gravity value
R : average radius of the earth
H : elevation of survey point (m)

Bouguer correction value Δg_2 is obtained according to the following formula, taking the immensely broad plate of the thickness of H and with the density of ρ to be inserted between the surface and the geoid.

$$\Delta g_2 = -2\pi G\rho H \fallingdotseq -0.0419\rho \times H \text{ mgals}$$

Here symbols stand for

G : gravity constant

ρ : density

H : elevation of survey point (m)

Both free-air correction value and bouguer correction value are functions of elevation of survey point, H. They are called elevation correction values collectively, and are calculated by the following formula.

$$\Delta g_1 + \Delta g_2 = (0.3086 - 0.0419\rho)H$$

3-1-5 Latitude correction

By the facts that the earth is an ellipsoid of revolution and that centrifugal force is brought about by the earth's revolution, smallest gravity value appears along the equator while the highest value is observed at the poles. Latitude correction values are obtained by deducting standard gravity values (S.V.) from the measured gravity values. The standard gravity values are calculated according to the international formula of the standard gravity values (1930) as shown below.

$$\text{S.V.} = 978{,}049(1 + 0.0052884 \sin^2\varphi - 0.0000059 \sin^2 2\varphi) \text{ mgals}$$

Here φ : latitude of survey point

3-2 Density measurement of rock samples

Measurement of density of rock samples was carried out under wet condition and under naturally dried condition.

The density under natural dry condition (ρ_1) is obtained according to the following formula.

$$\rho_1 = w_o/(w_o - w_s)$$

Here symbols stand for

w_o : weight in air

w_s : weight in water

Also, the density under wet condition (ρ_2) is obtained according to the following formula.

$$\rho_2 = w_o/(w_o - w_s)$$

w_s : weight in water after soaking the material for more than 48 hours.

w_o : weight in air, left for one hour after measurement of wet density, with surface moistures wiped off.

3-3 Compilation

To obtain a gravity map, the data of the present gravity survey, was compiled with the data which had been obtained by DMR.

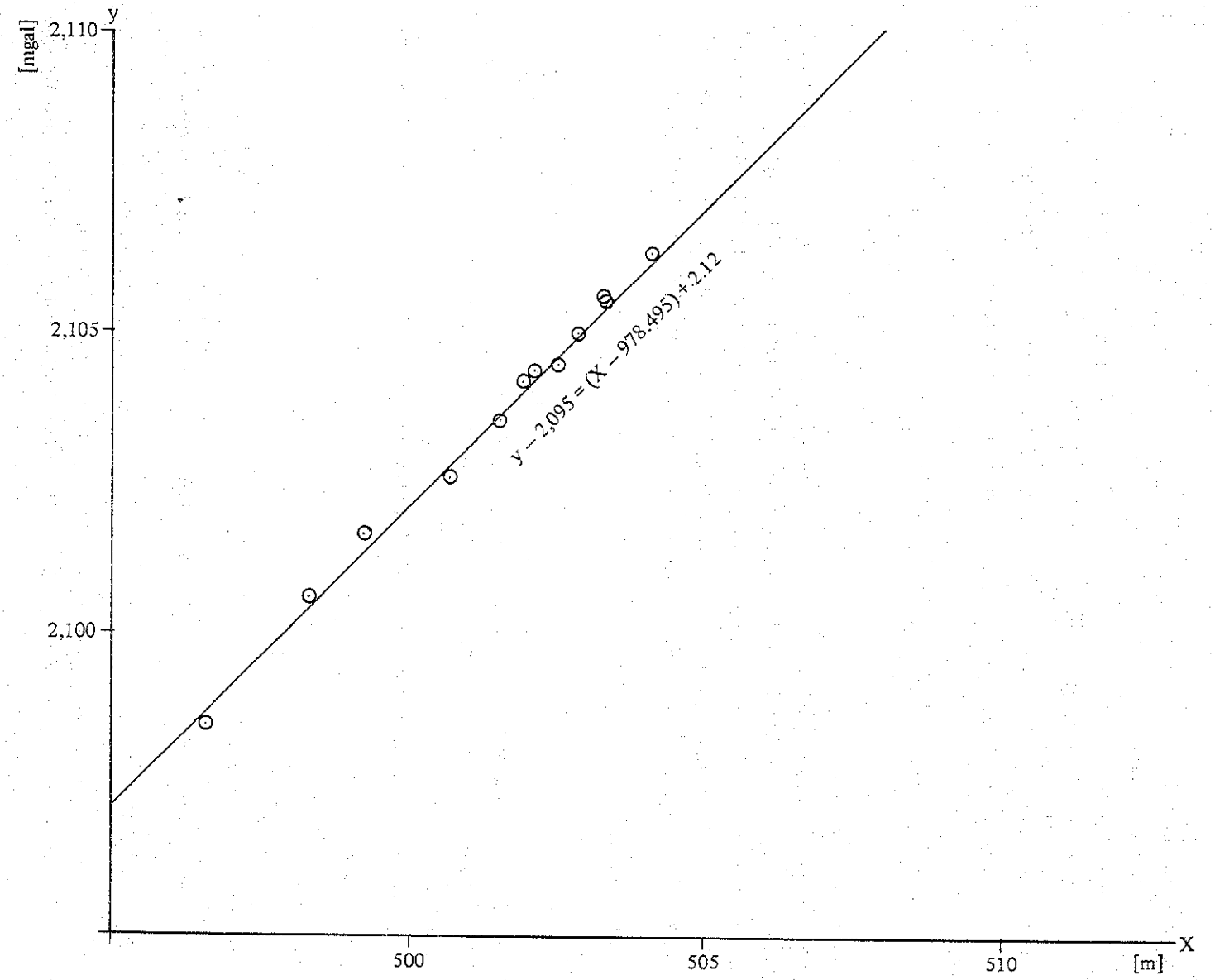

Fig. II.1.2-10 Gravity compile relation

Table II.1.2-4 Calculation of compile coefficient

	New sounding point		Old sounding point			Difference of altitude ① − ③ (m)	Difference of gravity value ② − ④ (mgal)
No.	① Altitude (m)	② Gravity value (mgal)	No.	③ Altitude (m)	④ Gravity value (mgal)		
27	390.119	978,499.210	A 35	400.895	2,101.162	−10.776	976,398.048*
54	360.633	501.877	A 22	370.649	2,104.151	−10.016	397.626
80	364.650	504.088	B 59	375.628	2,106.334	−10.978	397.754
86	379.185	502.404	R 16	389.810	2,104.427	−10.625	397.977
103	383.516	500.653	B 12	394.533	2,102.583	−11.017	398.070*
105	375.092	502.804	B 17	385.758	2,104.983	−10.666	397.821
108	383.700	498.399	B 26	396.692	2,100.444	−12.992*	397.955
109	383.900	501.503	H 2	394.400	2,103.506	−10.500	397.997
113	385.946	502.048	B 73	396.496	2,104.359	−10.550	397.689*
118	374.764	503.212	B 64	385.531	2,105.598	−10.767	397.614*
120	361.397	503.255	B 56	372.290	2,105.477	−10.893	397.778
124	370.784	498.294	A 6	380.181	2,100.602	− 9.398*	397.692*
140	416.003	496.558	A 49	426.556	2,098.484	−10.553	398.074*
221	383.037	502.463	O 1	393.962	2,104.434	−10.925	398.029
Average of difference altitude and difference of gravity value					$\bar{x}_0$	$\bar{x}_0 = -10.761$	$\bar{x}_0 = 976,397.873$
Standard deviation					σ_{n-1}	$\sigma_{n-1} = 0.7712$	$\sigma_{n-1} = 0.1637$
Average without data of * mark					$\bar{x}$	$\bar{x} = -10.689$	$\bar{x} = 976,397.880$

As for the Thailand side data, the control point of the gravity was not clear and the location of the survey points was not certain. By linking the survey points with survey data by Thailand side on the location map of the survey points, shapes of the former survey routes were drawn up. Thus, with the comparison of these shapes to the route maps along the roads in the present survey, the Thailand side survey points were estimated and located.

The tidal correction by Thailand side was done straightly by the base tie carried out every half a day, and it is thought that error of the degree of maximum 0.1 m gals could possibly be included.

In the gravity survey by the Thailand side, the elevations of the survey points were obtained by the level survey. But as the datum point is different from that of the present survey, the elevation is different even if the former survey point is thought to be at the same point as the present point.

Considering these problems, compilation was carried out by preparing compilation coefficient by the correlation of the data of the present survey points and of the thailand side survey points which were thought to be at the same location as the present survey points. The results of the correlation and the calculation of the compilation coefficient are shown in Fig. II.1.2-10 and in Table II.1.2-4. The figures with * mark are those far from the average value by more than the standard deviation σ_{n-1}. As this is thought to have been caused by fairly large difference of location, the compilation coefficient was calculated by eliminating these marked values. The compilation coefficients are as follows.

for values of level survey, $\overline{X} = -10.689$ m
for values of gravity, $\overline{Y} = 976{,}397.880$ mgals

Applying these compilation coefficients to the data of the gravity survey by Thailand side, these data were employed in the compilation of the present gravity survey.

At the stage to draw up iso-gravity map, the data at the survey points, where iso-gravity contour lines were distorted remarkably, were excluded, by the estimation that it would have been caused by the accumulation of several errors. Of the Thailand side data of the survey points, those close to the present survey points and those out of the designed surveyed area were excluded. The total number of the compilation points were 87, finally.

3-4 Determination of correction density

Correction density is quite important, as it has significant influence to the results of analysis. In the present survey, the average density was calculated by the following three methods, and the correction density was determined from the results of such calculation.

3-4-1 Method by density measurement of rock samples

The results of the measurement of the density of the collected rock samples are displayed in the Table II.1.2-5 and in the Fig. II.1.2-11 (a).

The densities of the rock samples are distributed in as wide range as 1.96 to 3.05 g/cm^3. The average of the average densities of respective lithological units is 2.65 g/cm^3.

Of the individual lithological unit, values of density measurement of chert, shale and tuff are quite scattering, while only small scattering is observed with those of sandstone, granite and quartz veins.

Table II.1.2-5 Measurement result of rock density (1)

Rock	No.	Weight in wet state		
		Weight in air (g)	Weight in water (g)	Density (g/cm^3)
Basalt	20	1469.9	971.9	2.95
〃	21	1769.9	1171.6	2.96
〃	22	417.4	279.2	3.02
〃	23	795.6	503.2	2.72
〃	24	1418.1	927.2	2.89
〃	25	723.4	472.2	2.88
〃	26	1072.5	715.7	3.01
〃	27	1280.4	839.0	2.90
〃	28	1645.6	1095.2	2.99
〃	29	873.6	573.4	2.91
〃	30	847.1	563.9	2.99
〃	81	1069.3	707.6	2.96
〃	82	1181.7	787.5	3.00
Tuff	1	1558.5	1003.8	2.81
〃	2	1201.9	770.9	2.79
〃	3	1092.6	702.8	2.80
〃	4	1109.1	734.4	2.96
Basaltic tuff	5	1268.0	829.6	2.89
Tuff	6	675.8	454.3	3.05
〃	7	1199.6	771.2	2.80
〃	8	1790.3	1202.7	3.05
〃	9	1997.1	1326.0	2.98
〃	10	1032.4	682.4	2.95
〃	11	840.4	562.6	3.03
〃		322.1	194.0	2.51
Tuff breccia	12	1033.7	679.2	2.92
〃	13	1020.3	667.5	2.89
〃	14	1204.0	781.2	2.85
〃	15	1493.6	979.8	2.91
〃	16	902.7	600.5	2.99
〃	17	1191.5	798.0	3.03
〃	18	1544.5	1028.1	2.99
〃	19	598.3	396.8	2.97
Limestone	52	394.5	250.0	2.73
〃	53	690.8	435.5	2.71
〃	54	1648.0	1034.9	2.69
〃	55	1783.2	1136.8	2.76
〃	56	741.1	465.1	2.69
〃	57	461.3	290.0	2.69
〃	58	524.5	330.0	2.70
Silicified limestone	83	1267.5	782.7	2.61
Limestone	59	1060.6	667.5	2.70
〃	60	1024.1	648.1	2.72
〃	61	1255.0	792.1	2.71
〃	62	498.5	319.8	2.79
〃	63	903.5	572.2	2.73
Chert	47	305.2	164.2	2.16
〃	48	1175.3	707.8	2.51
〃	49	1105.2	666.1	2.52
〃	50	998.6	598.3	2.49
〃	51	545.7	338.3	2.63

Table II.1.2-5 Measurement result of rock density (2)

Rock	No.	Weight in wet state		
		Weight in air (g)	Weight in water (g)	Density (g/cm^3)
Calcareous shale	31	451.6	281.6	2.66
Black shale	32	451.6	281.6	2.66
Shale	33	1373.7	807.9	2.43
Calcareous shale (fresh)	34	743.5	468.5	2.70
〃 (weathered)	35	1406.2	852.9	2.54
Shale	36	602.2	375.7	2.66
Black shale	79	736.1	455.1	2.62
Shale	84	672.9	385.5	2.34
〃	37	691.8	438.0	2.73
〃	38	1307.9	816.9	2.66
Weathered shale	39	388.4	190.3	1.96
Sandstone	40	696.0	427.7	2.59
〃	41	641.8	396.3	2.61
〃	42	655.2	394.6	2.51
〃	64	528.5	321.0	2.55
〃	65	237.3	145.6	2.59
〃	66	367.5	226.5	2.61
〃	67	1312.3	807.1	2.60
〃	43	567.3	337.2	2.47
〃	68	1436.7	886.6	2.61
〃	78	1198.9	727.0	2.54
〃		848.2	523.3	2.61
〃	80	1094.5	659.6	2.52
〃	44	1162.9	694.4	2.48
〃	45	1265.3	777.2	2.59
〃	46	1156.3	698.5	2.53
〃	69	825.3	496.6	2.51
Granite	70	233.3	145.2	2.65
〃	71	1574.5	954.5	2.54
〃	72	1075.9	649.8	2.52
Quartz vein	73	696.0	427.7	2.59
〃	74	1330.9	812.5	2.67
〃	75	1024.0	629.7	2.60
〃	76	968.0	592.0	2.57
〃	77	1161.1	724.8	2.66

Geological age	Geological unit		Lithology	Amount	Average of density (g/cm²)	
Permian	Kiu Lom Formation	Upper	Basaltic tuff Tuff breccia Lapilli tuff	19	2.93	2.93
			Basalt	13	2.94	
		Middle	Shale	11	2.54	2.59
			Sandstone	9	2.54	
			Chert	5	2.46	
			Limestone	13	2.71	
Carboni-ferous	Mae Tha Forma-tion		Sandstone	6		2.58
Triassic			Granite	3		2.57
			Quartz vein	5		2.62

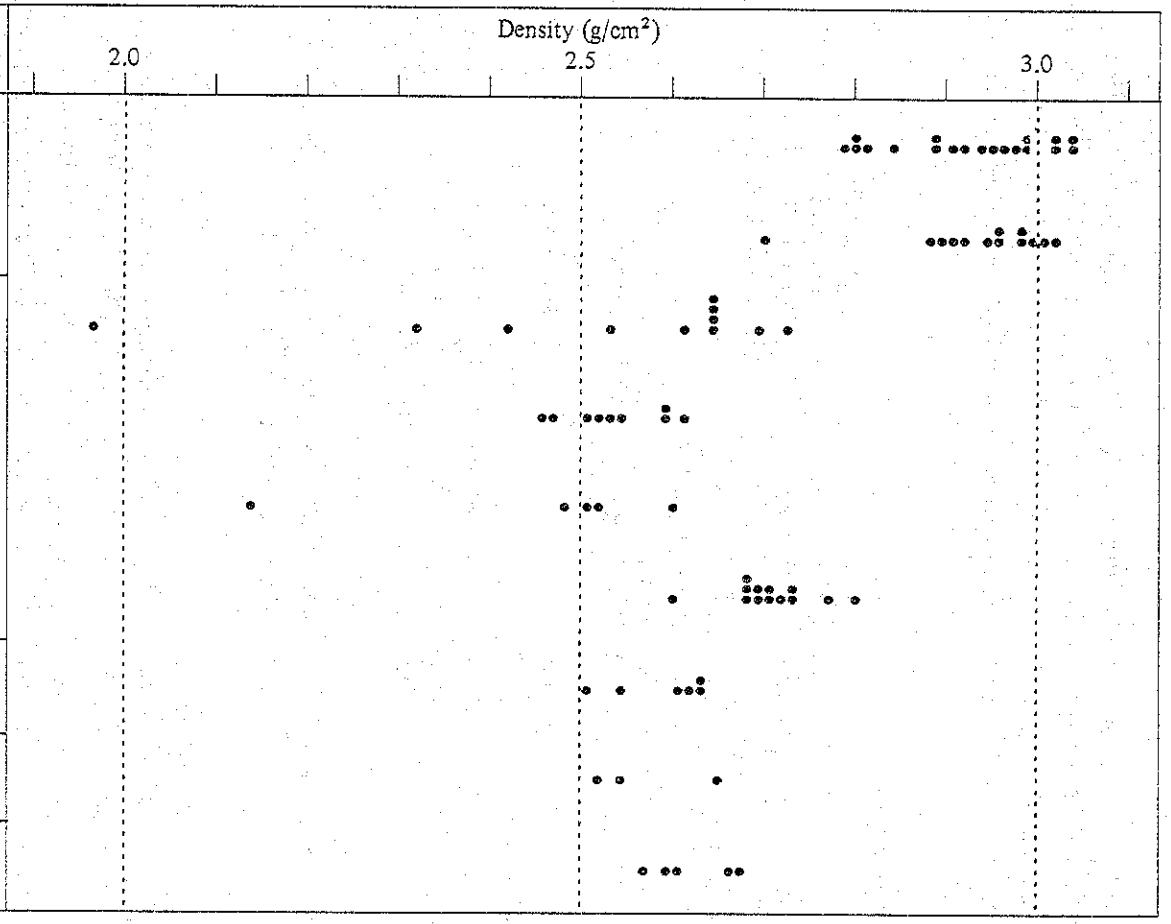

Fig. II.1.2-11(a) Distribution of rock densities

As for the high density area, the basaltic tuff, tuff breccia and lapilli tuff of the upper part of the Kiu Lom Formation were revealing high density values, followed by limestone. Density of chert is generally small.

From the above results, the rock densities in the surveyed area are divided as shown below.

			g/cm³
High Density			
	The upper part of the Kiu Lom Formation	basaltic tuff, tuff breccia, lapilli tuff	2.93
		basalt	2.94
Medium Density			
	The middle part of the Kiu Lom Formation	limestone	2.72
	The Mae Tha Formation	sandstone	2.58
	other	granite	2.57
		quartz vein	2.62
Low Density			
	The middle to lower part of the Kiu Lom Formation	shale	2.56
		sandstone	2.54
		chert	2.46

Accordingly, it is thought to be appropriate that the correction density in this surveyed area based on the density measurement of the rock samples is 2.5 ~ 2.9 g/cm³.

3-4-2 Method by G-H relation

The method by G-H relation is that to obtain correction density from the relation that elevation of every survey point has linear correlation [$\Delta G = (0.3086 - 0.04199) \times \Delta H$] with gravity value after terrain correction and latitude correction, where underground structure is homogeneous. However, the gravity values after the correction in this present survey was thought to contain anomalous values derived from the heterogeneous underground structure. Therefore, after obtaining trend surface of third order polynomial to eliminate influences by large scale underground structure, G-H relation was plotted by the residual values. The G-H relation is shown in Fig. II.1.2-11 (b). From the gradient of the G-H relation, the average density can be calculated directly to be $\rho = 2.614$ g/cm³ in this surveyed area.

3-4-3 Method by correlation of the topographical contour lines to the iso-gravity countour lines by the various correction

Iso-gravity map after terrain correction and bouguer correction has no correlation to topographical countour lines, when the topography is not related to underground structure. If correction density is too small compared to appropriate value, iso-gravity conter lines have similar trend to that of the topographical contour lines, while iso-gravity map has the lowest correlation to topographical map when correction density is quite big compared to appropriate value. The results of the consideration on the above points are given in Table II.1.2-6. From the data shown in this table, it is possible to regard the density of $\rho = 2.6$ g/cm³ to be the most appropriate density value.

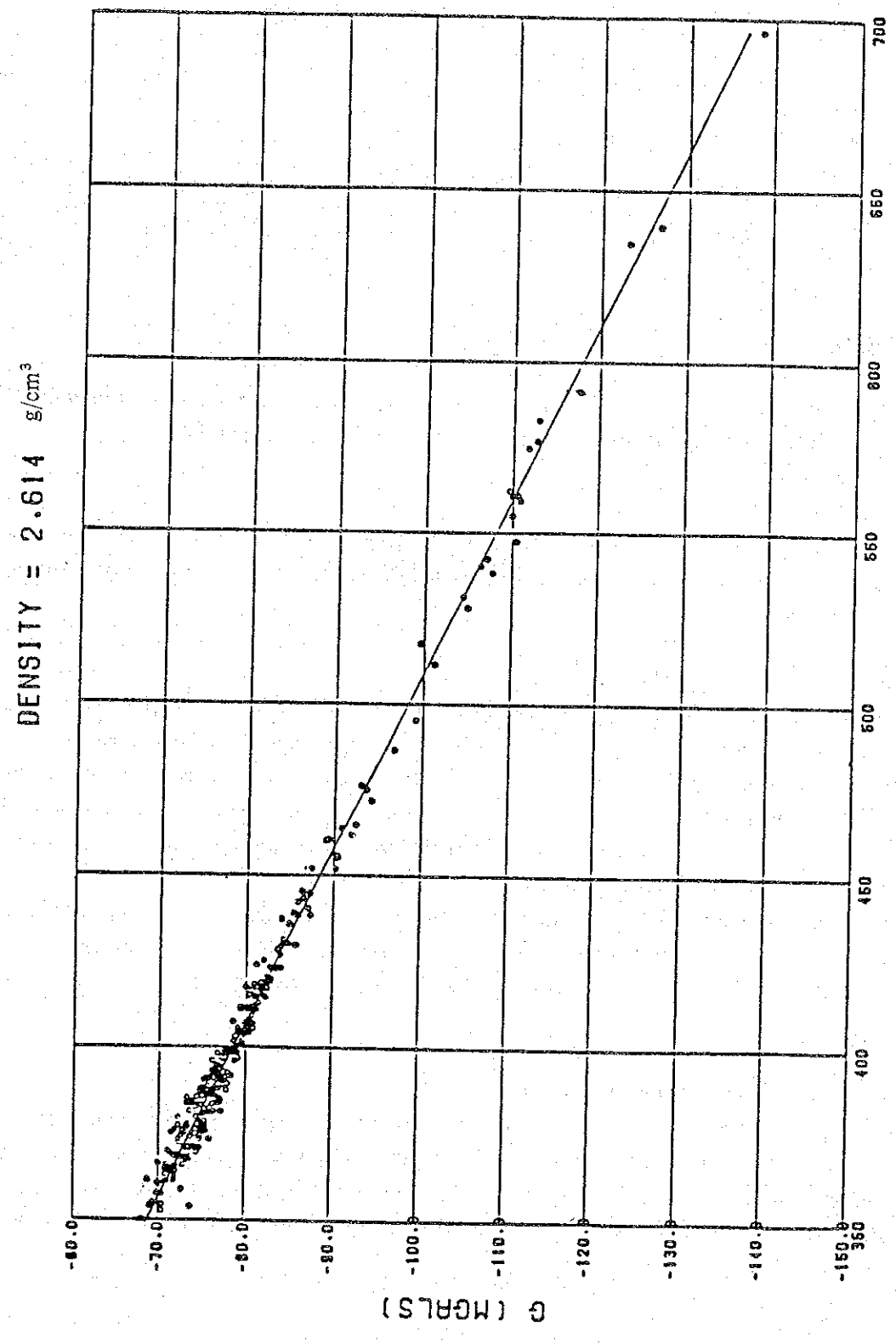

Fig. II.1.2-11 (b) G–H relation

From the results of the three considerations as above mentioned, the correction density was established to be ρ = 2.6 g/cm^3.

Table II.1.2-6 Correlation of the iso-gravity map

(g/cm^3)	ρ=2.4	ρ=2.5	ρ=2.6	ρ=2.67	ρ=2.8
Number of locations where correlation is positive	11	10	8	7	5
Number of locations where correction is negative	4	6	9	10	14

3-5 Iso-gravity map

The iso-gravity map was prepared and drawn in the following processes.

First of all, concerning the measured data and the respective survey points for compilation, corrected gravity values are calculated by the method stated in the paragraph 3-1.

3-6 Filter treatment

As the iso-gravity map contains various wave lengths caused by various elements, the following filtering treatment was applied to the extraction of necessary informations as to the underground structure.

3-6-1 Trend surface analysis of third order polynomial

The trend surface analysis of the third order polynomial is a method to extract average trend of the whole of the surveyed area through mathematical treatment. The result obtained is thought to expressed such gravity anomalies as brought by large scaled structure including the surrounding areas and the geological structure at the depth. This filtering treatment is a method to obtain residual gravity map stated in the following paragraphs. The residual gravity map can be a gravity map at the objective level for the analysis.

The trend surface analysis of third order polynomial is an analysis to obtain approximated curved surface, expressed by third order polynomial through the method of least squares on the gravity values at the grid point. The results of the analysis is shown in PL. II.1.2-2 (Gravity trend).

3-6-2 Residual gravity map of third order polynomial

The map of the residual gravity of third order polynomial is drawn up by reducing gravity values on the trend surface of third order polynomial from gravity values at the grid points on the gravity anomaly map. The relation of gravity value at the grid point G(X,Y), gravity value on the trend surface of third order polynomial Z(X,Y) and the residual gravity of third order polynomial is shown as follows.

$$\text{Residual gravity} = G(X,Y) - Z(X,Y)$$

3-6-3 Spectrum analysis

Spectrum analysis is an analysis to get information on the depth of principal structures by the

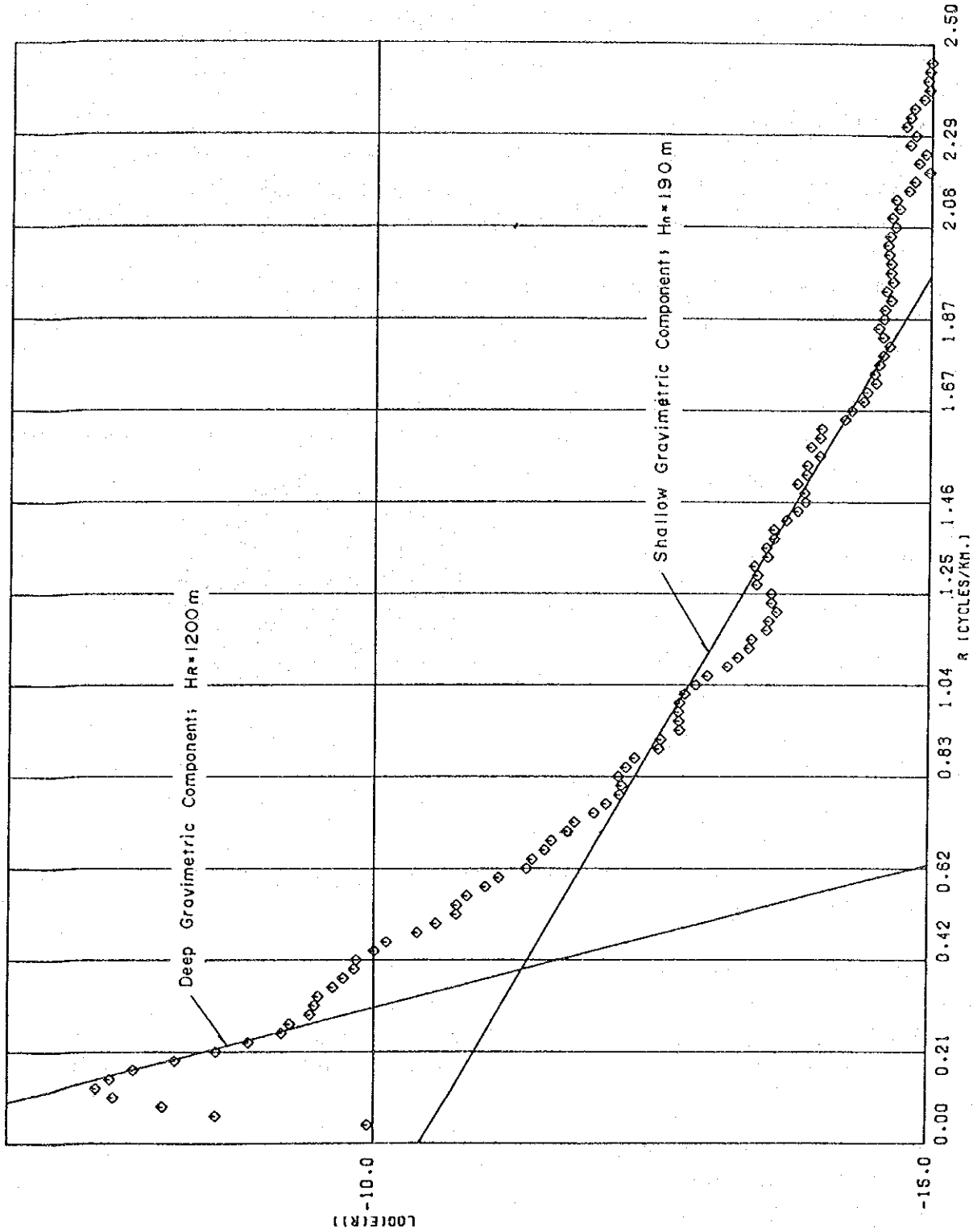

Fig. II.1.2-12 Spector analysis

analysis of wave length, based on the potentiality theory. Magnetic gravity and magnetism are expressed in potential, and the analysis of wave length can be applied directly. By this method, were drawn up Spectrum analysis (Fig. II.1.2-12), Deep gravimetric component (average depth: 1,200 m) (PL. II.1.2-4) and Shallow gravimetric component (average depth: 190 m) (PL. II.1.2-5).

3-7 Profile analysis

In order to estimate underground structure corresponding to the gravity anomalies, profile analysis was carried out, employing values of the primary residual gravity.

For the calculation of gravity values for density structure model, Talwani's method is employed.

Vertical component g_v of the gravity at a point 0 (an arbitrary point on the surface) brought by polygon (infinitely vertical to the sheet) of the density of ρ, as shown in Fig. II.1.2-13, is given by the following formula.

$$g_v = 2\rho G \sum_{i=1}^{n} \int_{z_i}^{z_{i+1}} \int_{\infty}^{x} \frac{Z}{X^2 + Z^2} dx \cdot dZ$$

Here ρ: density
G: gravity constant

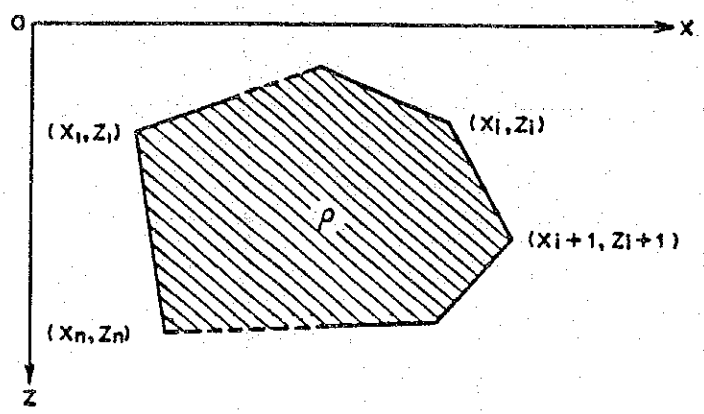

Fig. II.1.2-13 Profile analysis

The profile analysis was performed with the three profiles of A – A', B – B' and C – C', the location of which are shown on the PL. II.1.2-1.

4. Result of the analysis

4-1 Plans and profiles of analysis

By the analysis as shown in the paragraph 3, the following plans and profiles have been drawn up.

PL. II.1.2-1 Bouguer Anomaly (ρ = 2.6 g/cm^3)
PL. II.1.2-2 Gravity Trend
PL. II.1.2-3 Residual Gravity
PL. II.1.2-4 Deep Gravimetric Component (1,200 m)
PL. II.1.2-5 Shallow Gravimetric Component (190 m)
PL. II.1.2-6 Underground Structure (A – A')
PL. II.1.2-7 Underground Structure (B – B')

PL. II.1.2-8 Underground Structure (C – C')
PL. II.1.2-9 Underground Structure

4-1-1 Bouguer anomaly (ρ = 2.6 g/cm^3) (PL. II.1.2-1)

The highest value of the isogravity countour is –2.25 mgals, while the lowest value of that is –12.25 mgals.

The trend of the iso-gravity countours is N-S as a whole. Especially, in the east end, in the central part and in the west end of the surveyed area, crowded distribution of the N-S trend iso-gravity contours is remarkable. In these areas, existence of the faults are estimated by the geological survey, such as the Huai Mae Koen fault, the Huai Mae Khu Ha fault, the Ban Mae Khu Ha fault and the Huai Pong fault.

The area from around Ban Mae Khu Ha to around Ban On Klang is between the east end and the central part of the surveyed area with clustered iso-gravity contours. The area composes high gravity zone, where iso-gravity contours are roughly distributed. In this area, are distributed basalt, basaltic tuff, tuff breccia and lapilli tuff belonging to the upper part of the Kiu Lom Formation. It is thought that the density of the rocks of these beds varues little.

The central area where iso-gravity contours are closely clutsered extends far in north and south direction. Here the above-stated Huai Mae Khu Ha fault is located. The limestone of the middle part of the Kiu Lom Formation, which is distributed in the west side of this fault, is situated at the western end of the area with the closely clustered iso-gravity contours found in the central area. The strike of the limestone beds and the trend of those iso-gravity contours are well corresponding.

The area from around Ban Norg Boyen to around Ban Pong Nok is between the central area and the western end of the surveyed area, in both of which iso-gravity contours are closely crowded. The area composes low gravity zone, where iso-gravity contours are roughly In this area, shale, chert and sandstone of the middle to lower part of the Kiu Lom Formation are distributed. The area where the geothermal indications are distributed is in the low gravity anomaly zone extending in north and south, but along the northern side of this area, the iso-gravity contours are trending in the direction of WNW-SES.

The western margin of this block is in contact with sandstone of the Mae Tha Formation bounded by the Huai Pong fault. The gravity values increase in the western area of this fault and the iso-gravity contours are crowded a little closer one another.

4-1-2 Gravity trend (PL. II 1.2-2,3)

The highest values of the iso-gravity contours is +2.0 mgals, while the lowest value of that is –2.0 m gals. The gravity distribution is divided into units of the scale of 3 km in diameter.

As for high gravity anomalies in the area where the basalts are distributed in the east of the Ban Mae Khu Ha fault, there is an anomaly near Huai Mae Khu Ha extending in NW-SE direction. Also in the area southward from the EGAT camp and around Ban Mae Pa Khang, there is an anomaly extending in N-S direction.

There are high gravity anomalies extending in NW-SE direction, around Ban Kat Khi Lek along the northern extension of the Huai Pong fault and in the east of Doi Luang where sandstone of the Mae Tha Formation is distributed.

Low gravity anomalies are distributed around Ban Mae Khu Ha, around Ban Pang Riap Rua in

its northwest, along Huai Ang River and around Wat Hua Fai.

4-1-3 Deep gravimetric component (average depth: 200 m) (PL. II.1.2-4)

The highest value of the iso-gravity contour is 7.0 mgals while the lowest value of that is −6.75 mgals. It is thought that forms appeared in this Deep gravity component map are the result of fair influence from the geological structure in the intermediate depth between that shown on the Gravity trend map and that shown on the Residual gravity map.

The high gravity anomalies are located in almost same areas as shown on the Gravity trend map and on the Residual gravity map. The bow-like shape of the iso-gravity contours closely crowded in the area between the high gravity anomaly and the low gravity anomaly in the eastern part of the surveyed area is corresponding well to the distribution of limestone.

The low gravity anomalies are located in the west of the area where they are on the Residual gravity map. The centers of the low gravity anomalies are distributed in an area from Wat Pon Hong to around Ban Pon Nok where the Kiu Lom Formation is found the around the Huai Pong fault near the Huai Ang River.

4-1-4 Deep gravimetric component (average depth: 190 m) (PL. II.1.2-5)

The highest value of the gravity anomaly is 0.4 mgals and the lowest values is −0.9 mgals. The variation is extremely small. Borrespondence of forms and distribution of the anomalies to the geology is uncertain. It is thought that they would reveal density noises of the shallow part in the underground.

4-1-5 Underground structure by profiles (PL. II.1.2-6,7,8)

The subject profiles include iso-gravity profiles, filter profiles, underground structure profiles and geological profiles.

The iso-gravity profile has been prepared by plotting the results of the two dimensional simulation on the iso-gravity profile of the correction density of ρ = 2.6 g/cm^3 (bouguer anomaly).

The filter profile expresses the results of third order polynomial residual gravity and spectrum analysis (deep gravimetric component).

The underground structure profile expresses the structural model by the results of the simulation.

The geological structure profile expresses geological structure estimated by adding geological information on the surface to the above-mentioned results of analysis.

The density structure obtained by the simulation is divided, common to the respective profiles, into the high density mass (ρ = 2.80 g/cm^3), the low density mass (ρ = 2.50 g/cm^3, 2.60 g/cm^3) and the middle density mass (ρ = 2.7 g/cm^3).

The high gravity anomaly in the eastside of the center of the profile is elucidated by the existence of the high density mass (ρ = 2.80 g/cm^3), which is in contact vertically with the low density masses (ρ = 2.60 g/cm^3).

Although the gravity values are increasing in the western end of the respective profiles, the density model was prepared with homogeneous density of ρ = 2.60 g/cm^3, as the information was not sufficient for density calculation.

The low gravity anomaly in the western part of the profiles can be elucidated by the

existence of the low density mass (ρ = 2.60 g/cm^3 and ρ = 2.49 g/cm^3). In the area with steep gravity gradient in the central part the profiles, forms of the medium density mass (ρ = 2.70 ~ 2.64 g/cm^3) obtained by the subject gradient interpretation are different in each profile. It is thought by this interpretation that, in the A–A′ profile and in the B–B′ profile, big volume of the medium density mass is expected from the gentle gravity gradient, while small volume of the medium density mass is expected in the C–C′ profile viewing from its most steep gravity gradient. Correspondence of the density mass to the geological beds is thought to be as shown in the Table II.1.2-7.

Table II.1.2-7 Correspondence of density mass to geology

Profile / Density mass	A – A′	B – B′	C – C′
ρ=2.8	Upper part of the Kiu Lom Formation	Upper part of the Kiu Lom Formation	Upper part of the Kiu Lom Formation
ρ=2.7	Middle to lower part of the Kiu Lom Formation		
ρ=2.66		Middle to lower part of the Kiu Lom Formation	
ρ=2.6 (eastside)	Kiu Lom Formation (shale)	Lower part of the Kiu Lom Formation (shale)	Lower part of the Kiu Lom Formation (sandstone)
ρ=2.6 (westside)	Middle to lower part of the Kiu Lom Formation	Middle to lower part of the Kiu Lom Formation	Middle to lower part of the Kiu Lom Formation
	Mae Tha Formation (sandstone)	Mae Tha Formation (sandstone)	Mae Tha Formation (sandstone)
ρ=2.49	Lower part of the Kiu Lom Formation (chert)	Lower part of the Kiu Lom Formation (chert)	
ρ=2.64			Lower part of the Kiu Lom Formation (chert)

As for the iso-gravity profile, calculation of simulation was repeated to seek the most appropriate values by varying the forms and the densities of the density masses, after primary model was prepared by the geological profile and the results of the density measurement. The iso-gravity profile was drawn with the most appropriate values thus obtained. Therefore, the final iso-gravity profile is in harmony with the geological profile.

4-2 Gravity distribution and underground structure (PL. II.1.2-9)

The underground structure in the surveyed area is divided into the following four blocks of [I], [II], [III] and [IV], by the boundary of large scaled faults or tectonic lines, viewing from the gravity distribution.

[I] block ; the area east of the Huai Mae Koen fault

[II] block ; the area from the Huai Mae Koen fault to the area where the limestone bed in the middle part of the Kiu Lom Formation is distributed.

[III] block ; the area from the above limestone bed to the Huai Pong fault
[IV] block ; the area west of the Huai Pong fault and the Doi Luang fault

In the [I] block, shale of the Kiu Lom Formation and sandstone of the Mae Tha Formation are widely distributed. This block is represented by low gravity anomaly by the difference of the density of the above rocks from that of the basaltic rocks which are distributed in the west of this block. The dense distribution of the iso-gravity contours found near the Huai Mae Koen fault is thought to be revealing that the fault composes the boundary of different density masses. From the profile analysis, it is estimated that the Huai Mae Koen fault is vertical.

In the [II] block, the basaltic rocks belonging to the upper part of the Kiu Lom Formation are distributed. It is thought that the variation of the densities in the basaltic rocks is small, as the interval of the iso-gravity contours is moderate. Also, from the profile analysis, the thickness of the beds is estimated to be large. The density of the basaltic rocks, $\rho = 2.93$ g/cm^3, is the highest of the rocks found in the surveyed area and the high gravity anomaly extending is N-S direction is formed with the basaltic rocks.

In this block, the Huai Wai fault, the Huai Mae Khu Ha fault and otwer faults crossing the former two are distributed. However, except for the southern part of the Huai Mae Khu Ha fault, these faults have no influence on the gravity distribution. The densitic boundary with the [III] block is formed by the Huai Mae Khu Ha fault in the southern half of the block, while in the northern half it is represented by a fault oblique to the Huai Mae Khu Ha fault. This oblique fault is observed to extend from near the point of the geothermal exploration well GTE-3 to around Ban Pan Riap Rua, in NW-SE direction. The Huai Mae Khu Ha fault is almost vertical while this oblique fault is estimated to be dipping to the east from the results of the profile analysis.

The [III] block is located in the west side of the [II] block, as far to the Doi Luang fault, and is characterized by low gravity zone. This [III] block is further divided into blocks of [III-1], [III-2] and [III-3], from east to west, by the Ban Mae Khu Ha fault and the Huai Pong fault. In the [III-1] area, basaltic rocks are distributed on the surface, as is seen in the [II] block, but the gravity value have tendency to be lower gradually toward the west. By the profile analysis, the density of the [III-1] area is $\rho = 2.66 \sim 2.70$ g/cm^3, which is lower than that of the [II] block of $\rho = 2.80$ g/cm^3.

In the [III-2] area located in the west side of the Ban Mae Khu Ha fault, sedimentary rocks such as sandstone, shale and chert are distributed. The densities of these rocks are the lowest in the surveyed area, and it is from the difference of the densities of the rocks distributed in the [II] block and in the [IV] block that the low gravity anomaly appears in this area.

By the Trend surface map, further lower gravity anomaly is found in the low gravity zone of the [III] block, and existence of a fault of WNW-ESE trend is estimated there. This lower gravity anomaly extends in an area of 1.5 km by 2 km from near GTE-2 to the area where the basalts are distributed in the [III-1] area.

The [III-3] area occupies an area between the Doi Luang fault composes density boundary rather clearly than the Huai Pong fault. In this [III-3] area, sandstone of the Mae Tha Formation is distributed.

The [IV] block is in contact with the [III] block, bounded by the Huai Pong fault in the northern part and by the Doi Luang fault in the south. The sandstone in the [IV] block, belonging to the Mae Tha Formation has a little higher density than that of the sedimentary rocks of the Kiu Lom Formation, it is thought that the [IV] block is found to reveal higher gravity

anomaly compared to the [III] block. The Doi Luang fault in the southern part composed density boundary. The higher gravity anomaly relative to the [III] area is expressed in the [IV] block in the west of this fault. By this gravity distribution step-like faults are thought to exist here.

5. Summary

(1) The gravity survey was carried out with the cooperation of Thailand side counterpart, EGAT and DMR, and with the joint of students of the Khon Khaen University, as a part of their field practice. Level survey was performed by EGAT crew with whole of the survey points. Number of the total survey points in the present gravity survey is 230. Compilation works were carried out with 87 data of the former gravity survey which had already been conducted by the Thailand side. Number of the rock samples for the density measurement is 84.

(2) Values of gravity anomalies were calculated after various correction such as tidal correction, drift correction and datum correction. Iso-gravity contour map was drawn based upon the values thus obtained.

The survey points were located by land survey with simplified transit compass, in addition to the utilization of the survey lines byh EGAT.

(3) The most appropriate value of the correction density for the gravity contour map was determined to be $\rho = 2.6$ g/cm^3, by the density measurement of the collected rock samples, by the G-H relation and by the correlation of the topographical map with the gravity map by various corrections of density.

(4) Various filter treatments were completed with the bouguer anomaly map ($\rho = 2.6$ g/cm^3) and profile analysis was done with three profiles.

(5) Trends of the bouguer anomaly map ($\rho = 2.6$ g/cm^3) are N-S, NW-SE and NE-SW, principally, which are well correspondent with the strikes of the beds and the faults confirmed in the geological survey.

(6) By the results of the analysis, the followings have been disclosed.

1. Viewing from the results of the density measurement and from the gravity distribution, the basaltic rocks of the upper part of the Kiu Lom Formation are to compose high density mass to be corresponding to high gravity anomaly, while the sedimentary rocks such as sandstone, shale and chert of the middle to lower part of the Kiu Lom Formation are to compose low density mass to be corresponding to low gravity anomaly.
2. The surveyed area is divided into the following four blocks by the density distribution as shown in the underground structure map (PL. III.1.2-9).

[I] block ; Area east of the Huai Mae Koen fault

[II] block ; Area from the the Huai Mae Koen fault to the area where the limestone bed in the middle part of the Kiu Lom Formation is distributed.

[III] block ; Area from the above limestone to the Huai Pong fault.

[IV] block ; Area west of the Huai Pong fault and the Doi Luang fault.

3. It is thought that the density boundary dividing the [I] block and the [II] block is in N-S trend, vertical and correspondent to the Huai Mae Koen fault.
4. The thickness of the basaltic rocks distributed in the [II] block has been estimated to be more than 2 km, by the result of the profile analysis.
5. The [III] block is further divided into two sub-areas by the Ban Mae Khu Ha fault; the area where the basaltic rocks are distributed in the east of the fault, and the area where the sedimentary rocks are distributed in the west of the fault. Low residual gravity anomaly has been found around this Ban Mae Khu Ha fault.
6. In the [IV] block, sandstone of the Mae Tha Formation is distributed. By the correlation of the gravity distribution in this block to that in the [III-3] area, existence of step-like faults is estimated.

(7) The [III] block, which includes the area where the geothermal indications are distributed, is correspondent to the low gravity anomaly. In this area of the low anomaly, there is a low gravity zone of the residual gravity of third order polynomial.
In the [III] block, the basaltic rocks and the sedimentary rocks are distributed, bounded by the Ban Mae Khu Ha fault. The chert bed found around the area where the geothermal indications are distributed is dipping to the east, which is toward the center of the low gravity zone. It seems that the low gravity zone is surrounded by the limestone bed which is found along its eastern margin. Many faults are estimated there and in the vicinity. It is thought that numerous fractures and fissures were concentrated in the area represented by this low gravity zone, formed in the period of the tectonic movement.